Pflugers Arch - Eur J Physiol (2016) 468:1333–1352
DOI 10.1007/s00424-016-1835-4

Evidence for the functional involvement of members of the TRP channel family in the uptake of Na^+ and NH_4^+ by the ruminal epithelium

Julia Rosendahl[1] · Hannah S. Braun[1] · Katharina T. Schrapers[1] · Holger Martens[1] · Friederike Stumpff[1]

Received: 11 January 2016 / Revised: 14 March 2016 / Accepted: 4 May 2016 / Published online: 17 May 2016

Abstract Large quantities of protein are degraded in the fermentative parts of the gut to ammonia, which is absorbed, detoxified to urea, and excreted, leading to formation of nitrogenous compounds such as N_2O that are associated with global warming. In ruminants, channel-mediated uptake of NH_4^+ from the rumen predominates. The molecular identity of these channels remains to be clarified. Ruminal cells and epithelia from cows and sheep were investigated using patch clamp, Ussing chamber, microelectrode techniques, and qPCR. In patch clamp experiments, bovine ruminal epithelial cells expressed a conductance for NH_4^+ that could be blocked in a voltage-dependent manner by divalent cations. In the native epithelium, NH_4^+ depolarized the apical potential, acidified the cytosol and induced a rise in short-circuit current (I_{sc}) that persisted after the removal of Na^+, was blocked by verapamil, enhanced by the removal of divalent cations, and was sensitive to certain transient receptor potential (TRP) channel modulators. Menthol or thymol stimulated the I_{sc} in Na^+ or NH_4^+ containing solutions in a dose-dependent manner and modulated transepithelial Ca^{2+} fluxes. On the level of messenger RNA (mRNA), ovine and bovine ruminal epithelium expressed TRPA1, TRPV3, TRPV4, TRPM6, and TRPM7, with any expression of TRPV6 marginal. No bands were detected for TRPV1, TRPV5, or TRPM8. Functional and molecular biological data suggest that the transport of NH_4^+, Na^+, and Ca^{2+} across the rumen involves TRP channels, with TRPV3 and TRPA1 emerging as prime candidate genes. TRP channels may also contribute to the transport of NH_4^+ across other epithelia.

Keywords Ammonium · TRP channel · Rumen · Climate gas · Menthol · Thymol

Introduction

Rising emissions of ammonia represent an urgent problem of global dimensions that is associated with eutrophication, climate change, and direct dangers to humans [53]. Livestock are estimated to account for almost 50 % of global ammonia emissions, cattle alone for about 30 % [8, 12]. The greater part of these ammonia emissions are related to the rapid microbial degradation of dietary protein into ammonia, with the amounts absorbed exceeding 20 mol·day^{-1} in high yielding animals [15]. Although a variable percentage of the urea that is formed can be recycled to the gut, large quantities are renally excreted and thus lost as a source of nitrogen for microbial protein synthesis [23, 52]. Furthermore, absorption of ammonia from the gastrointestinal tract can lead to life-limiting complications in human patients suffering from hepatic or renal disease [22]. A better understanding of the mechanisms of ammonia transport is thus necessary.

Typically, the permeability of most cellular membranes to ammonia is high so that until recently, the uptake was thought to occur via simple diffusion. However, the NH_3 molecule is highly polar, and today, there is little doubt that membrane proteins such as Rh-glycoproteins [34, 61, 66] and aquaporins [11, 37, 46] are involved in mediating membrane transport of NH_3. In addition, the protonated form, NH_4^+, can substitute for K^+ in essentially every known K^+ transporting protein, facilitated by the strikingly similar biophysical properties of the two cations [62].

✉ Friederike Stumpff
stumpff@zedat.fu-berlin.de

[1] Institute of Veterinary Physiology, Faculty of Veterinary Medicine, Freie Universität Berlin, Oertzenweg 19b, 14163 Berlin, Germany

In the case of the rumen, ammonia uptake does not drop with pH as might be expected, and accordingly, the lipid diffusion model has been critically discussed for many decades [10, 18]. Past studies have shown that at the pH found physiologically in the rumen (<6.8), channel-mediated uptake of NH_4^+ greatly exceeds efflux in the form of NH_3 [1] and efflux of protons via this pathway may contribute to ruminal pH homeostasis [4]. The purpose of the current study was to identify candidate genes for this conductance. In particular, we tested the response of the native epithelium to a number of monoterpenoids. These compounds are known for their highly specific interaction with channels of the transient receptor potential (TRP) channel family [14, 40], famously allowing mammals to distinguish between the fragrance of a multitude of herbal compounds in a highly selective manner [42, 60].

The TRP multigene superfamily consists of 28 known sequences that are subdivided into seven subfamilies, six of which are found in mammalian tissues: TRPC (canonical), TRPV (vanilloid), TRPM (melastatin), TRPP (polycystin), TRPML (mucolipin), and TRPA (ankyrin) [41]. These genes encode for integral membrane proteins consisting of six transmembrane spanning segments, the assembly of which as homotetramers or heterotetramers results in the formation of cation-selective channels [39, 43]. Channels of this family were initially identified in sensory organs [36], where various stimuli including light, heat, cold, or odorants lead to an opening of the channels with influx of Ca^{2+} and Na^+ [42, 60]. However, it is increasingly emerging that TRP channels also play important functional roles in many nonsensory tissues [39]. Thus, TRPV5 and TRPV6 are highly selective for Ca^{2+} and mediate the renal and intestinal transport of this cation [27, 58], while TRPM7 is involved in the Mg^{2+} homeostasis of multiple tissues including the ruminal epithelium [50]. We now additionally report ruminal expression of the epithelial Mg^{2+} channel TRPM6, which plays a decisive role in renal Mg^{2+} transport [27].

In the current study, we present functional and molecular biological evidence for the involvement of either TRPV3 or TRPA1 or both in the transport of Na^+, NH_4^+, and Ca^{2+}. To our knowledge, evidence for the involvement of TRP channels in the transport of NH_4^+ has not been reported previously and may more generally provide clues for the function of these channels in epithelial transport.

Methods

Ruminal epithelium

All animals were slaughtered in accordance with German laws for the protection of animals (TierSchG) at a commercial slaughterhouse. Removal of tissue occurred some 15 min after death, after which it was immediately stripped and transported to the laboratory (~1 h) in a warm (37 °C) and gassed (95 % O_2/5 % CO_2) transport buffer containing (in mmol·l^{-1}) the following: 115 NaCl, 25 $NaHCO_3$, 0.4 NaH_2PO_4, 2.4 Na_2HPO_4, 5 KCl, 5 Glucose, 1.2 $CaCl_2$, and 1.2 $MgCl_2$ (pH~7.4) [33]. For cell culture, tissues were transported in ice-cold buffer, isolated via trypsination and cultured as in previous studies [17, 20].

Chemicals and modulators

All chemicals were obtained from Carl Roth (Karlsruhe, Germany) or Sigma-Aldrich (Taufkirchen, Germany). Commercially unavailable salts such as *N*-methyl-D-glucamine (NMDG)–gluconate or NH_4^+–gluconate were produced by titrating NMDG or ammonia with gluconic acid to a pH of 7. $^{45}Ca^{2+}$ for the flux measurements was obtained from Hartmann Analytic (Braunschweig, Germany). All channel modulators used in the study were protected from light and solved in DMSO or ethanol so that the desired concentration could be reached by dilution with the appropriate buffer at a ratio of 1:1000. All channel modulators were stored at −20 °C or prepared freshly and kept on ice until immediately before use.

Patch clamp experiments

All whole cell patch clamp experiments were performed with an EPC9 amplifier using TIDA or Patchmaster software with automatic offset potential, capacitance, and series resistance correction (HEKA Elektronik, Lamprecht, Germany) [20, 55]. A DMZ-Universal-Puller (Zeitz-Instruments, Munich, Germany) was used to pull pipettes to a resistance of ~4 to 5 MΩ. The bath chamber was continuously perfused with solutions at room temperature. Cations flowing into the pipette correspond to a negative current.

Pipette solutions contained (in mmol·l^{-1}) either 122 Na–gluconate or 122 K–gluconate, to which was added: 15 NaCl, 5 KCl, 1 NaH_2PO_4, 0.9 $MgCl_2$, 5 EGTA, and 10 Hepes (pH 7.2/Tris). Bath solutions contained either 137 NaCl, $NMDG^+$–gluconate, or NH_4^+-gluconate in a background of 5 KCl, 1 NaH_2PO_4, 1.7 $CaCl_2$, 0.9 $MgCl_2$, and 10 Hepes (pH 7.4/Tris). In NH_4–gluconate EDTA solution, $CaCl_2$ and $MgCl_2$ were replaced by 5.2 NMDGCl and 5 EDTA. All solutions were adjusted to 300 mosmol·l^{-1} using mannitol.

Current kinetics were observed at a sampling rate of 5 kHz; changes in current amplitude were monitored continuously at 100 Hz between −120 and +100 mV from a holding potential of −40 mV (Fig. 1a). In the tables, the current at +100 mV (designated as I_{100}) and the current at −120 mV (designated as I_{-120}) are given normalized to capacitance. Reversal potentials (U_{Rev}) were calculated via linear regression around 0 pA and corrected for liquid junction potential [6, 7]. Relative permeability ratios (P_x/P_y) were calculated for each cell from the

corrected reversal potential $E_{rev,X}$ and $E_{rev,Y}$ in solutions "X" and "Y" using:

$$E_{rev,\,X} - E_{rev,Y} = -\frac{R \cdot T}{F} \cdot \ln\left(\frac{P_X \cdot [X]_o}{P_Y \cdot [Y]_o}\right) \quad (1)$$

$[X]_o$ and $[Y]_o$ represent the concentrations of the ion X and Y in the bath, P_X and P_y the corresponding permeability, while R, T, and F have their usual meanings [24]. Alternately, an estimate for the relative permeability ratio P_x/P_y between the major cation in the pipette solution (with concentration $[Y]_i$) and in the bath (with concentration $[X]_o$) was obtained from the Goldman-Hodgkin-Katz equation by neglecting the (relatively small) contribution of the other cations and anions so that:

$$E_{rev,\,X} = -\frac{R \cdot T}{F} \cdot \ln\left(\frac{P_X \cdot [X]_o}{P_Y \cdot [Y]_i}\right) \quad (2)$$

Microelectrode experiments

Bovine ruminal tissue was placed, apical side up, in a small horizontal microelectrode chamber that was perfused continuously with warm (37 °C) and gassed (O_2) solution [55]. The transepithelial voltage (PD_t) and short-circuit current (I_{sc}) were measured via voltage clamp (Biomedical Instruments, Munich, Germany) and recorded via Lab Chart 7 Pro (v. 7.3.3) for Windows (AD Instruments, Bella Vista, NSW, Australia). Conductance was monitored briefly by a 10-mV voltage pulse before each solution change.

Double-barreled pH-sensitive microelectrodes (for measuring PD_a and intracellular pH (pH_i)) were used to measure intracellular parameters via a FDA Dual Electrometer (World Precision Instruments, Sarasota, FL, USA) as previously described in [33]. A majority of impalements rapidly collapsed and only those recordings in which PD_a returned to the original level ±15 % at the end of the experiment were

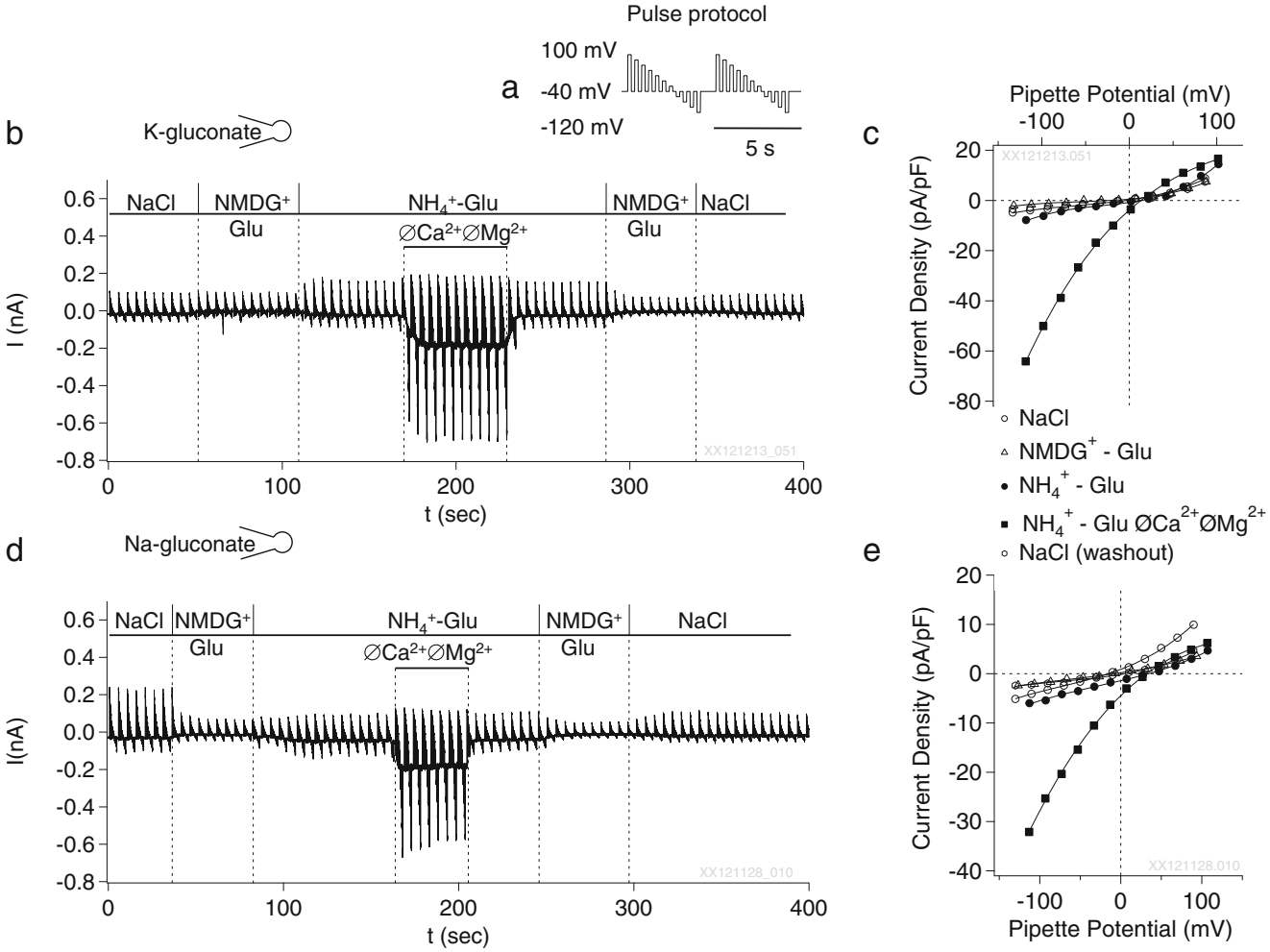

Fig. 1 Original whole cell recordings of bovine ruminal epithelial cells exposed to the continuous pulse protocol depicted in **a**. Cells were filled with K–gluconate pipette solution (**b**) or Na–gluconate pipette solution (**d**). Cations flowing into the cell generate a negative current that is depicted in the figures as going downward. The solutions in the bath were consecutively changed as indicated. Exposure to NH_4^+ resulted in a stimulation of both inward current at −120 mV and outward current at +100 mV, with further enhancement by a removal of divalent cations ($\varnothing Ca^{2+}$ $\varnothing Mg^{2+}$). All changes were essentially reversible upon washout. The corresponding current–voltage relationships are given in **c** and **e**

chosen for evaluation. All signals were referenced to the apical side (SE 21-L, Sensortechnik Meinsberg, Germany) so that a positive I_{sc}, PD_t, or PD_a reflects a movement of cations from the apical to the serosal side [32]. To allow an easier comparison with patch clamp measurements, in which an opposite sign convention is used, positive currents reflecting inward currents of cations into the tissue are depicted in figures as going downward.

For experiments, all solutions were gassed with 100 % O_2 and warmed to 37 °C by an inline solution heater before introduction to the perfusion chamber. The serosal buffer contained (in mmol·l^{-1}) the following: 70 NaCl, 0.4 NaH_2PO_4, 2.4 Na_2HPO_4, 5 KCl, 30 Na–gluconate, 1.2 $MgCl_2$, 1.2 $CaCl_2$, 2.5 glutamine, 40 NMDGCl, and 5 glucose, adjusted to pH 7.4 (8 MOPS). The mucosal side of the tissue was superfused with variable solutions with a pH of either 7.4 or 6.4 (8 MES) ("standard NaCl buffer", pH 7.4 or pH 6.4). In addition, two mucosal NH_4Cl solutions (pH 7.4 and 6.4) were used in which 40 mmol·l^{-1} NMDGCl was replaced by an equimolar amount of NH_4Cl ("standard NH_4^+ buffer", pH 7.4 or pH 6.4). In some experiments, the standard NaCl buffer was altered by replacing 70 mmol·l^{-1} NaCl in the buffer above by an equimolar amount of NMDGCl, resulting in a buffer designated as "Na^+-free" that contained 110 mmol·l^{-1} NMDGCl. As before, 40 mmol·l^{-1} NMDGCl was replaced by NH_4Cl to yield a NH_4^+-containing buffer ("NH_4^+-buffer, Na^+-free"). In solutions designated as divalent cation free, $CaCl_2$ and $MgCl_2$ were replaced by 5 mmol·l^{-1} EDTA. All solutions were adjusted to 300 mosmol·l^{-1} using mannitol.

TRP channel modulators were pipetted directly into the 50-ml storage containers at the end of the thin silicon tubing leading to the perfusion manifold so that no switch in the perfusion lane was required. Since these containers were strongly bubbled with 100 % O_2, mixing was very rapid.

Flux experiments in Ussing chambers

Tissues of ovine origin, in which a separation of the ruminal mucosa from the submucosal layers is much easier than in the bovine species, were mounted in Ussing chambers, resulting in an exposure area of 3.14 cm^2 [1]. Chambers contained 16 ml of serosal or mucosal buffer, and were circulated by a gas lift system (5 % CO_2/95 % O_2). The serosal solution contained (in mmol·l^{-1}) the following: 70 NaCl, 0.4 NaH_2PO_4, 2.4 Na_2HPO_4, 5 KCl, 40 Na–gluconate, 1.2 $MgCl_2$, 1.2 $CaCl_2$, 25 $NaHCO_3$, 5 glucose, and 8 MOPS (pH 7.4). The mucosal buffer contained 70 NaCl, 0.4 NaH_2PO_4, 2.4 Na_2HPO_4, 5 KCl, 25 Na-acetate, 10 Na-propionate, 5 Na-butyrate, 1.2 $MgCl_2$, 1.2 $CaCl_2$, 25 $NaHCO_3$, 5 glucose, and 8 MES (pH 6.4). The agonist or solvant was directly pipetted to the mucosal side of the tissue 25 min after the beginning of the experiment.

All measurements were conducted in short-circuit mode (Mussler Scientific Instruments, Aachen, Germany). Transepithelial conductance G_t was determined from a 100-μA current pulse and monitored throughout. As above, the equivalent short-circuit current I_{sc} represents the negative of the current required to clamp potential to zero, so that cations transported from the apical side to the basolateral side produce a positive $I_{sc} = PD_t \times G_t$ that is represented in figures as going downward.

To allow a direct comparison between the I_{sc} value and the expected conductance G correlated to this flux of ions, the molar flux J (given in μeq·cm^{-2}·h^{-1}) was calculated from the total flux Φ_t of ions (in A·cm^{-2}) using Faraday's constant ($F = 96\ 485$ A·s^{-1}·mol^{-1}) and:

$$J = \Phi_t / F \cdot 3600\ \mathrm{s \cdot h^{-1}} = \Phi_t / 26.80\ \mu\mathrm{eq \cdot cm^{-2} \cdot h^{-1}} \quad (3)$$

According to Nernst diffusion theory [24, 25], the conductance (G_t) can be calculated from the corresponding flux of ions (Φ, in amperes):

$$G_t = F \Big/ (R \cdot T)\ \cdot \Sigma \Phi_i \cdot z_i = \Phi_t \Big/ (26.7mV) \quad (4)$$

Since at 310 K (37 °C) and by sheer coincidence, the conversion factor of 26.8 is thus almost exactly identical to R·T/F = 26.73 mV, a tissue conductance of 1 mS·cm^{-2} reflects an ion flow of ≅1 μeq·cm^{-2}·h^{-1}.

$^{45}Ca^{2+}$ (45 kBq per 16-ml chamber) was added to either the mucosal or serosal side ("hot"). Starting 100 min after the beginning of the experiment, three flux periods of 30 min each were measured by taking a sample from the opposite "cold" side. The sample volume was then replaced by corresponding buffer. Radioactivity was measured using a β-counter (LKB Wallace-Perkin-Elmer, Überlingen, Germany). Ouabain was added serosally at the end of the experiment (final concentration 100 μmol·l^{-1}) to block the Na^+/K^+-ATPase. Tissues were considered to have passed this vitality test if I_{sc} dropped by more than 0.05 μeq·cm^{-2}·h^{-1} within 10 min.

For analysis, epithelia from the same animal were paired after sorting for G_t values. Data from tissues that did not pass the vitality test were rejected, as were flux data that were more than twice the size of other fluxes in the treatment group. All tissues paired to such epithelia were also excluded, so that only complete sets with data from the same animal in each treatment group were evaluated. The net calcium flux ($J_{net}(Ca^{2+})$) was calculated from the difference between mucosal to serosal flux ($J_{ms}(Ca^{2+})$) and serosal to mucosal flux ($J_{sm}(Ca^{2+})$) for paired epithelia.

Molecular detection of TRP channels in ruminal epithelial tissue

Ruminal samples from six lactating cows and two sheep were taken immediately after slaughter, rinsed and stripped from the outer muscular layers. Pieces of approx. 1 cm^3 were transferred into RNA*later*® (Ambion, Austin, TX, USA) filled 1-ml tubes and stored at −70 °C. For total RNA isolation, a Nucleospin RNA II Kit was used (Macherey&Nagel, Dueren, Germany), including a DNAse digestion step. RNA integrity numbers (RINs) of the samples were checked using a lab-on-a-chip technique (RNA 6000 n Kit, Agilent, Waldbronn, Germany) to ensure a RIN > 7. An iScript® cDNA synthesis kit (Bio-Rad Laboratories, Munich, Germany) was applied according to the manufacturer's instructions to perform reverse transcription by using 1 μg of RNA of each sample. Reactions were diluted 1:10. For polymerase chain reaction (PCR) experiments, three samples were subsequently pooled.

Intron-spanning primer pairs were designed to detect the target genes TRPA1, TRPM6–M8, and TRPV1–V6 of both sheep and cattle according to the predicted sequences of both species (Primer3 software, http://bioinfo.ut.ee/primer3-0.4.0/primer3, for primer sequences see Table 1). Pooled complementary DNA (cDNA) (9.5 μl) was added to 12.5 μl *Taq* PCR Master Mix Kit (QIAGEN, Venlo, the Netherlands), with 1.5 μl of the forward and revers primer each (20 pmol). A 40-cycle two-step PCR protocol (30 s at 58 °C and 15 s at 94 °C) was performed on a thermocycler (Eppendorf, Hamburg, Germany). Reaction products were analyzed in a 1.5 % agarose gel electrophoresis, using Midori Green Advanced DNA Stain (Biozym Scientific, Hessisch Oldendorf, Germany) to detect DNA bands under UV illumination. To ensure binding to the correct target, all amplicons were subsequently sequenced (GATC Biotech, Konstanz, Germany). To prevent false negative results, all primer pairs listed in Table 1 were successfully tested in control tissues (e.g., bovine medulla oblongata, kidney, or testis). TRPV2 was omitted since no staining was observed in any sample using two different pairs of primers.

For quantitative PCR (qPCR) experiments using SYBR green, intron flanking primer pairs for target genes TRPA1, TRPM6–M8, TRPV1, and TRPV3–V6 and the reference gene YWHAZ were designed as described above (for some

Table 1 Primer sequences and amplicon length of the target genes

Gene	Primers for PCR		Primers for qPCR	
	Primer PCR	Length (bp)	SYBR green	Dual labeled probes
TRPA1 fwd	tgtcacccttgttcatcagg	403	gatgatgtgaatgcctca	gatgatgtgaatgcctca
TRPA1 rev	atgaggacaattgggacgaa		ccacctggttttttcctgc	ccacctggttttttcctgc
TRPA1 probe				tgatggatgattacggaaataccccactgcac (FAM/BHQ1)
TRPV3 fwd	gtgcagatgctgatggagaa	265	gtgcagatgctgatggagaa	ctacaacaccaacattgacaac
TRPV3 rev	tgatctcacggctgagaatg		tgatctcacggctgagaatg	agcagaaggacaggaagaac
TRPV3 probe				cacacgctgctgcatatgaagtggaaga (FAM/BHQ1)
TRPM6 fwd	accatgaaaagccttggttg	339	acattggtctcctgcttc	
TRPM6 rev	cctggctgtccaaagacaat		acttttccacacactgttcttc	
TRPM7 fwd	ttggccagagtgaagcagtt	704	tcaacaggcaggaccttatg	
TRPM7 rev	ctttggtcggtagggctgt		caagagtccaagatggtg	
TRPM8 fwd	tgctgatcgacgtgttcttc	382	tgctgatcgacgtgttcttc	
TRPM8 rev	acctggtcgttgttttcctg		acctggtcgttgttttcctg	
TRPV1 fwd	cacgtacatcctcctgctca	255	cacgtacatcctcctgctca	
TRPV1 rev	gtgttccaggtggtccagtt		gtgttccaggtggtccagtt	
TRPV4 fwd	gacggggacctatagcatca	346	cgagatcatcacactcttcac	
TRPV4 rev	catgttaaggagcagcacga		gagacaatcaccagcacag	
TRPV5 fwd	gatgctggagaggaagatgc	384	gatgctggagaggaagatg	
TRPV5 rev	tgataaacccgatcgtctcc		tgataaacccgatcgtctcc	
TRPV6 fwd	gcacctttgagctgttcctc	275	gcacctttgagctgttcctc	
TRPV6 rev	aaacttgtgcccacagatcc		aaacttgtgcccacagatcc	
YWHAZ fwd			agagagaaaatagagaccgagc	agagagaaaatagagaccgagc
YWHAZ rev			agccaagtagcggtagtag	agccaagtagcggtagtag
YWHAZ probe				ccaacgcttcacaagcagagagcaaa (FAM/TAMRA)

target genes, the same primers could be used as in the PCR experiments). A 40-cycle two-step PCR protocol (30 s at 90 °C and 2 min at 58 °C) was performed on a thermocycler (iCycler IQ, Bio-Rad, USA) with 5 μl cDNA and three replicates per reaction. SYBR Green (IQ SYBR Green Supermix, Bio-Rad, USA) and primers were added according to the manufacturer's instruction in total assay volumes of 15 μl. Thresholds were automatically calculated by the cycler software. Dilution series-based gene-specific amplification efficiency was determined for every primer pair and subsequently included in the statistical evaluation. Negative controls (absence of template or retrotranscriptase) were routinely included. C_t values of all samples were cleared by the primer-specific amplification efficiency before target gene expression of each animal was related to the associated expression level of the reference gene YWHAZ.

In a second approach, the expression levels of the target genes TRPA1 and TRPV3, and the reference genes YWHAZ, RPS19, and β-actin were analyzed using self-designed gene-specific intron spanning primers and dual-labeled probes synthesized by Eurofins MWG Operon, Germany. A 40-cycle two-step PCR protocol (20 s at 60 °C and 1 s at 95 °C) was performed on a ViiA7 thermocycler (Applied Biosystems/Life Technologies, USA). Reactions were carried out in triplicates with 4.5 μl cDNA and iTaq® Universal Probes Supermix (Bio-Rad, USA) in a total assay volume of 10 μl. Thresholds were automatically set by the cycler software. As before, dilution series-based gene-specific amplification efficiencies were determined for every primer/probe pair; negative controls were again included routinely. Reference genes were examined for expression stability using the software qbasePLUS (Biogazelle NV, Zwijnaarde, Belgium). From the three reference genes tested, YWHAZ was recommended as the most stable and was therefore used to benchmark target gene expression within all samples. Mean target gene C_t values of six animals were averaged and calibrated to yield the mean C_t value of YWHAZ. Resulting relative expression levels were used for statistical analysis.

Statistics

All evaluations were carried out by using Sigma Plot program version 11.0 for Windows (Systat Software, San Jose, USA). Results are given as means ± SEM. P values of <0.05 were considered significant. N refers to the number of experimental animals, and n refers to the number of measurements on individual cells or tissues. Data were tested for normal distribution using the Kolmogorov–Smirnov test. Multiple comparisons were performed using one-way (repeated measures) analysis of variance (ANOVA) or ANOVA on ranks, as appropriate, followed by post hoc testing using the Student–Newman–Keuls (SNK) method to isolate the group or groups that differed from the others.

Results

Patch–clamp experiments

The purpose of the patch clamp experiments was to assess whether (a) cells of the bovine rumen express a conductance for NH_4^+ and (b) whether this conductance or part of it is modulated by divalent cations in a manner resembling the nonselective cation channel previously described [31, 49].

K–gluconate pipette solution

Cultured bovine ruminal epithelial cells were brought into the whole cell configuration and filled with a low calcium K–gluconate solution and consecutively superfused with various extracellular buffers (Table 2 and Fig. 1b, c). Mean capacitance was 35.60 ± 8.93 pF (n = 6). When NaCl in the bath was replaced by the largely impermeable NMDG, the current at −120 mV (I_{-120}) became less negative (p < 0.05), while the reversal potential dropped to a more negative value (p < 0.001), reflecting a decreased influx of cations. No significant effects on I_{100} were observed, which suggests that K^+-

Table 2 Summary of whole cell patch clamp data from primary cultures of bovine ruminal epithelial cells

Pipette	KGlu (n = 6)			NaGlu (n = 8)			p value NaGlu vs. KGlu		
Bath	U_{rev} (mV)	I_{-120} (pA·pF^{-1})	I_{100} (pA·pF^{-1})	U_{rev} (mV)	I_{-120} (pA·pF^{-1})	I_{100} (pA·pF^{-1})	U_{rev}	I_{-120}	I_{100}
NaCl	−19.18 ± 5.63 a	−4.92 ± 1.93 a	7.06 ± 1.99 a	−24.28 ± 5.99 a	−2.81 ± 0.91 a	7.74 ± 3.52 a	n.s.	n.s.	n.s.
NMDG-Glu	−44.08 ± 6.01 b	−3.52 ± 1.56 b	6.64 ± 2.19 a	−23.25 ± 12.13 a	−1.85 ± 0.74 b	3.12 ± 0.74 b	n.s.	n.s.	n.s.
NH4-Glu	4.45 ± 2.80 c	−12.9 ± 5.72 c	20.85 ± 3.64 b	22.75 ± 4.97 b	−4.17 ± 1.08 c	7.49 ± 2.14 a	<0.05	n.s.	<0.01
NH4-Glu EDTA	13.88 ± 0.83 c	−72.31 ± 13.7 d	26.29 ± 6.9 b	23.36 ± 1.60 b	−31.69 ± 8.0 d	9.85 ± 3.51 a	<0.01	<0.05	<0.05
NaCl (wash)	−14.44 ± 3.83 a	−13.36 ± 7.23 a	16.52 ± 5.42 c	−0.49 ± 4.49 c	−6.45 ± 4.75 a	10.41 ± 7.14 a	<0.05	n.s.	n.s.

Within columns, values with different lowercase letters are significantly different (p < 0.05, ANOVA, SNK). Means ± SEM

I_{-120} current density at −120 mV, I_{100} current density at +100 mV, U_{rev} reversal potential

efflux exceeded any influx of Cl^-. Subsequent replacement of extracellular $NMDG^+$ by NH_4^+ led to a more negative value of I_{-120} ($p<0.05$), while the reversal potential shifted into the positive range ($p<0.001$), with both changes reflecting an influx of NH_4^+. As previously seen [1], a simultaneous rise in I_{100} was observed ($p<0.05$). Since gluconate was used to replace chloride in the bath, this reflects enhanced efflux of K^+. Removal of Ca^{2+} and Mg^{2+} (NH_4–gluconate EDTA) induced a further reversible increase in the absolute size of I_{-120} to more negative values ($p<0.05$) and a slight rise in the reversal potential to more positive values ($p=0.07$), reflecting a further increase in the influx of NH_4^+. Any effects on I_{100} did not test for significance.

Relative permeability ratios according to Eq. 2 were $p(NH_4^+)/p(NMDG)=7.82\pm1.85$, rising to $p(NH_4^+$ (EGTA))/$p(NMDG)=11.57\pm2.57$ after removal of Ca^{2+} and Mg^{2+} ($p<0.001$). The reversal potential in NMDG–gluconate solution was used to calculate $p(K^+)/p(NMDG)=7.02\pm1.45$, which was not different from $p(NH_4^+)/p(NMDG)$ ($p=0.38$). Calculation of $p(NH_4^+)/p(K^+)$ from the reversal potential in NH_4^+–gluconate solution yielded a value of 1.14 ± 0.11.

Na–gluconate pipette solution

A further series of experiments was performed using a low calcium Na–gluconate pipette solution (Table 2 and Fig. 1d, e). Capacitance was 34.45 ± 5.01 pF ($n=8$). Since all ions except Ca^{2+} were in equilibrium across the membrane, the negative reversal potential reflects a significant contribution of chloride to total current [20, 55]. Accordingly, I_{100} was significantly reduced by the subsequent replacement of Cl^- by gluconate ($p<0.05$). Since simultaneously, Na^+ was replaced by $NMDG^+$, no significant effect on the reversal potential was observed. Again, replacement of NMDG–gluconate by NH_4^+–gluconate resulted in a more negative value of I_{-120} ($p<0.05$), while the reversal potential increased ($p<0.001$), suggesting an enhanced influx of NH_4^+ as before. The increase in I_{100} ($p<0.05$) suggests an increased efflux of Na^+ at +100 mV. Removal of Ca^{2+} and Mg^{2+} resulted in a further shift in I_{-120} to more negative values ($p<0.05$). The reversal potential remained the same due to a concomitant increase in the efflux of Na^+. Interestingly, the reversal potential was significantly higher after a return to the NaCl solution than at the beginning of the experiment ($p<0.05$), possibly reflecting a decrease in Cl^- conductance by the pretreatment with NH_4^+–gluconate.

Relative to NMDG, the permeability to NH_4^+ was $p(NH_4^+)/p(NMDG)=10.54\pm5.16$ and $p(NH_4^+$-EGTA)/$p(NMDG)=13.76\pm7.50$ ($p=0.64$). Both values did not differ from those found for K–gluconate filled cells. Calculation of $p(NH_4^+)/p(Na^+)$ from the reversal potential in NH_4^+–gluconate solution yielded a value of 2.84 ± 0.60.

Measurements with pH sensitive microelectrodes (open circuit mode, bovine rumen)

The response of the intact bovine ruminal epithelium to NH_4^+ was investigated by measuring the transepithelial potential, PD_t of the tissue in toto, and by measuring the apical potential PD_a and the intracellular pH (pH_i) of cells within the tissue via double-barreled pH-sensitive microelectrodes (Fig. 2 and Table 3). If ammonia enters the tissue primarily as NH_3, no effect on either PD_t or PD_a is expected, while pH_i should change toward a more alkaline value. Conversely, entry primarily in the ionic form as NH_4^+ should result both in changes in transepithelial and in apical potential.

To prevent interference with the measurement of PD_a, these experiments were performed in open circuit mode. However, brief voltage pulses of 10 mV were applied prior to every solution change to allow an assessment of transepithelial conductance G_t (arrow in Fig. 2).

PD_t

Measurements commenced with both sides superfused by standard NaCl buffer, pH 7.4. Lowering the apical pH to 6.4 had no effect on the PD_t ($\Delta PD_t=-0.01\pm0.08$ mV, $p=0.8$, N/n = 6/12), which only rose in response to addition of NH_4^+ (by $\Delta PD_t=+2.77\pm0.37$ mV, $p<0.05$, N/n = 6/12) (Fig. 2 and Table 3). In theory, this may reflect transport of NH_4^+. Alternately, NH_3 may induce changes in pH_i or cell volume with induction of currents mediated by other ions (e.g., Na^+ absorption or Cl^- secretion). For this reason, apical pH was subsequently increased to 7.4 in the continued presence of NH_4^+, which should increase the concentration of NH_3 by a factor of almost 10 with negligible impact on the concentration of NH_4^+. This maneuver had no impact on PD_t ($\Delta PD_t=+0.26\pm0.25$ mV, $p=0.3$, N/n = 6/12), arguing against effects of NH_3. Conversely, removal of NH_4^+ at pH 7.4 (standard NaCl buffer) rapidly led to a return of PD_t to values near the starting point ($\Delta PD_t=-2.53\pm0.12$ mV ($p<0.05$, N/n = 6/12)).

PD_a

Changes in the transepithelial potential can reflect a transfer of ions across the paracellular pathway, the transcellular pathway, or a combination of both. For this reason, the potential difference PD_a between the cytosol and the apical side was measured via an impaled microelectrode. Both at pH 6.4 and at pH 7.4, the PD_a was depolarized by application of NH_4^+ by $\Delta PD_a=2.12\pm0.50$ mV and $\Delta PD_a=2.18\pm0.40$ mV, respectively (both $p<0.05$, N/n = 6/12) (Table 3).

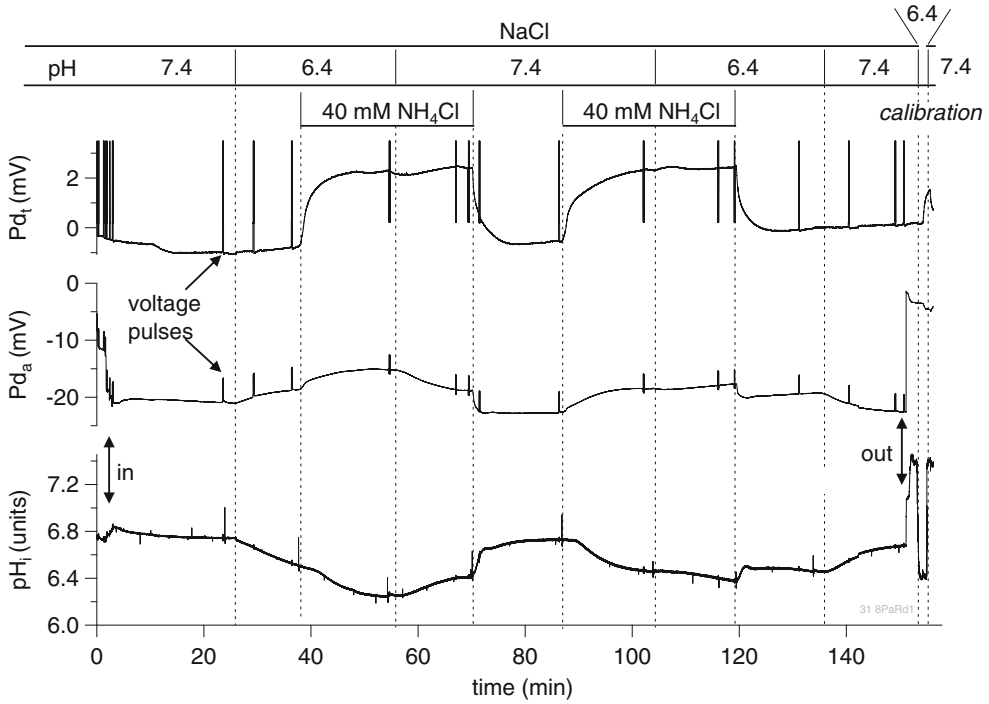

Fig. 2 Original recording from a measurement of native bovine ruminal epithelium in a continuously perfused horizontal microelectrode chamber. Before each change in solution, transepithelial tissue conductance was checked via brief voltage pulses (*arrows* in the figure). As the pH-sensitive microelectrode entered the tissue ("in"), PD_a could be seen to drop sharply from a value ~0 mV to ~−20 mV, while the pH remained essentially as in the microclimate formed by the stratum corneum covering the transporting epithelium. The tissue was subsequently exposed to various solutions in succession. At both pH 6.4 and pH 7.4, the PD_t and the PD_a were higher, the pH_i lower in solutions containing NH_4^+ than in control solutions at the same pH. At the end of the experiment, the microelectrode was completely withdrawn from the tissue ("out"), resulting in a sharp increase in PD_a to ~0 mV, while pH increased to ~7.4. Subsequently, the ion-selective microelectrode was recalibrated by switching the apical solution from pH 7.4 to pH 6.4 and back ("calibration")

pH_i

Reducing mucosal pH from 7.4 to 6.4 resulted in a significant intracellular acidification by $\Delta pH_i = -0.26 \pm 0.07$ ($p = 0.002$, N/n = 6/12) (Table 3). Apical exposure to standard NH_4^+ buffer at constant pH 6.4 led to a further significant drop of pH_i by $\Delta pH_i = -0.13 \pm 0.03$ ($p < 0.001$, N/n = 6/12). Effects were partially reversible after removing protons by switching to pH 7.4 ($\Delta pH_i = +0.23 \pm 0.07$ ($p = 0.009$, N/n = 6/12)). After removal of NH_4^+ and return to the standard NaCl buffer, pH_i increased by $\Delta pH_i = 0.18 \pm 0.05$, returning to the value at the beginning of the experiment ($p = 0.65$).

Table 3 Measurements of native bovine ruminal epithelium: transepithelial potential PD_t, apical potential PD_a, and intracellular pH_i

Mucosal solution	PD_t (mV)	PD_a (mV)	pH_i	N/n
NaCl 7.4	−0.11 ± 0.46 a	−13.92 ± 2.10 a	6.80 ± 0.05 a	6/12
NaCl 6.4	−0.10 ± 0.42 a	−14.10 ± 1.37 a	6.53 ± 0.07 b	6/12
NH_4Cl 6.4	2.68 ± 0.74 b	−11.97 ± 1.34 b	6.40 ± 0.06 c	6/12
NH_4Cl 7.4	2.42 ± 0.52 b	−12.91 ± 1.44 b	6.63 ± 0.06 b	6/12
NaCl 7.4	0.32 ± 0.47 a	−13.74 ± 1.67 a	6.81 ± 0.06 a	6/12

Values reflect means ± SEM of $n = 12$ tissues from $N = 6$ animals consecutively exposed to the solutions in column 1. All values were measured 10 min after the change to the respective solution. Within columns, values with different lowercase letters are significantly different ($p < 0.05$, ANOVA, SNK)

The short-circuit current across the bovine rumen: NH_4^+, bumetanide, verapamil, and divalent cations

The effect of 40 mmol·l^{-1} NH_4^+ on the transepithelial short-circuit current

In a second series of experiments, the short-circuit current (I_{sc}) necessary for clamping the transepithelial potential to 0 mV was measured without parallel impalement of the tissue, but in the same, continuously perfused microelectrode chamber as before. A switch from NaCl to standard NH_4Cl buffer (with 40 mmol·l^{-1} NH_4^+ instead of $NMDG^+$) led to a significant increase in I_{sc}, reflecting an absorption of cations. The effect was reversible upon washout (Table 4, Exp 1).

Table 4 Measurements of native bovine ruminal epithelium: short-circuit current (I_{sc}) (continuously perfused chamber)

Exp	Bath solutions			Short-circuit current I_{sc} (μA·cm^{-2})			N/n
	Solution 1	Solution 2	Solution 3	Solution 1	Solution 2	Solution 3	
1	NaCl	NH_4Cl	NaCl	2.43 ± 2.28 a	25.73 ± 2.14 b	2.68 ± 1.95 a	15/35
2	Na^+-free	NH_4Cl	Na^+-free	−20.84 ± 7.42 a	7.51 ± 6.64 b	−15.49 ± 7.53 a	4/10
3	NH_4Cl	NH_4Cl EDTA	NH_4Cl	16.18 ± 13.35 a	26.35 ± 15.28 b	19.36 ± 12.3 a	3/5
4	NH_4Cl	+1 mM Verapamil	NH_4Cl	21.22 ± 1.68 a	16.73 ± 1.53 b	20.51 ± 1.83 a	3/7

Each row represents means ± SEM from a series with consecutive application of solutions 1, 2, and 3, all measured 10 min after solution change. In Na^+-free buffers, NMDGCl was used to replace NaCl. Within rows, values with different lowercase letters are significantly different ($p < 0.05$, ANOVA, SNK)

The NH_4^+-induced current may reflect both transport of NH_4^+ in the ionic form or NH_4^+-induced contributions of other conductances (e.g. Na^+). Therefore, a further series of experiments was performed using Na^+-free NMDGCl buffers on the apical side. In this configuration, a negative I_{sc} was observed, possibly reflecting paracellular leak of Na^+ from the serosal to the mucosal side. Replacement of 40 mmol·l^{-1} NMDG by NH_4^+ again led to a reversible increase in I_{sc} (Fig. 3a and Table 4, Exp 2).

Bumetanide

In various epithelia of the gut, basolateral Na^+–K^+–$2Cl^-$ transport (NKCC) drives secretion of Cl^- which in turn modulates

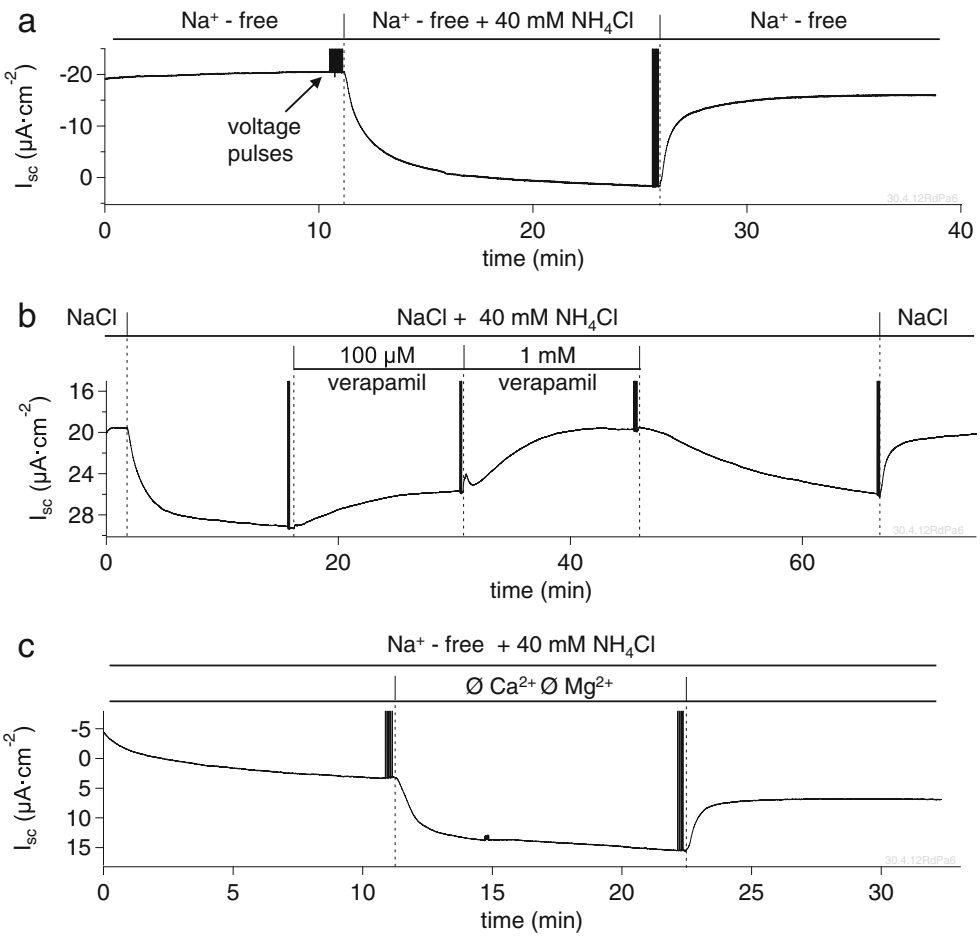

Fig. 3 Original recordings of ruminal epithelium. The same chamber was used as in Fig. 2, but PD_t was clamped to zero, so that the short-circuit current (I_{sc}) could be measured. As before, tissue conductance was checked via brief voltage pulses before each solution change. In analogy to the patch clamp experiments, positive currents reflecting an influx of cations into the tissue are depicted as going downward. **a** Replacing $NMDG^+$ by an equimolar amount of NH_4^+ in a Na^+-free solution induced a strong rise in I_{sc}, corresponding to movement of cations from the apical to the basolateral side (bovine rumen). **b** Currents could be partially blocked by verapamil (here: ovine rumen). **c** Removal of divalent cations enhanced the NH_4^+-induced current (bovine rumen)

the I_{sc}. Serosal application of the Na^+–K^+–$2Cl^-$ blocker bumetanide (100 μmol l^{-1}) to bovine rumen showed no effect (4.2 ± 0.65 to 3.74 ± 1.33 μA·cm^{-2}, ΔI_{sc} = 0.38 ± 0.85 μA·cm^{-2}, p = 0.7, N/n = 2/4).

The effect of verapamil and divalent cations

Verapamil blocks cation transport by various channels but not across the paracellular pathway. In standard NH_4^+ buffer (pH 6.4), verapamil reversibly blocked the current induced by NH_4^+ in bovine ruminal epithelium (ΔI_{sc} = −4.49 ± 0.93 μA·cm^{-2}, Table 4, Exp 4). In preparations from sheep, verapamil (1 mmol·l^{-1}) blocked current in standard NH_4^+ buffer (pH 6.4) by ΔI_{sc} = −10.73 ± 0.48 μA·cm^{-2} (p < 0.01, N/n = 2/4, from 42.91 ± 5.23 to 32.18 ± 5.02 μA·cm^{-2} with partial washout to 34.63 ± 4.34 μA·cm^{-2}) (Fig. 3b). At 100 μmol·l^{-1}, the blocking effects of verapamil were less clear (ΔI_{sc} = −2.92 ± 0.94 μA·cm^{-2}, p = 0.055, N/n = 2/5). The corresponding values were 40.62 ± 4.66 μA·cm^{-2} (NH_4^+) and 37.69 ± 4.30 μA cm^{-2} (NH_4^+ + 100 μmol·l^{-1} verapamil).

In analogy to the patch clamp experiments above, removal of Ca^{2+} and Mg^{2+} from the mucosal, Na^+-free NH_4^+ buffer resulted in a significant and reversible increase of the transepithelial current across bovine ruminal epithelium (Fig. 3c and Table 4, Exp 3).

The effect of various terpenoids on the I_{sc} across bovine rumen in NH_4^+ and Na^+ containing buffer solution

The previous results suggest that NH_4^+ may be conducted by the same divalent sensitive, nonselective cation channels that are also involved in the transport of various cations such as Na^+, K^+, Rb^+, and Cs^+ across the ruminal epithelium [30, 31, 49]. For further characterization, fragrant monoterpenoids that are known to interact with TRP channels of olfactory epithelia were added to the mucosal side of the tissue [60]. The serosal side of the epithelium was superfused with the standard NaCl buffer (pH 7.4) during all experiments.

Effect of menthol on NH_4^+-induced currents

Menthol is known to modulate the activity of TRPM8 [5], TRPV3 [59], and TRPA1 [28]. The mucosal addition of 1 mmol·l^{-1} menthol to the standard 40 mmol·l^{-1} NH_4^+ containing buffer led to a transient increase of the transepithelial current by ΔI_{scPeak} = 4.53 ± 0.94 μA·cm^{-2} (N/n = 3/12; p = 0.002). After this peak, current level dropped continuously, so that 10 min after washout, current level had dropped to a level that was ΔI_{scWash} = −7.84 ± 2.42 μA·cm^{-2} below that measured initially (N/n = 3/12; p = 0.085) (Fig. 4a and Table 5, Exp 1). Given in isolation, the solvent alone (ethanol) had no effect. Effects of 200 μmol l^{-1} menthol were similar, with current transiently rising by ΔI_{scPeak} = 5.35 ± 0.97 μA·cm^{-2} (N/n = 4/11; p = 0.006) before subsequently dropping by ΔI_{scWash} = −9.92 ± 2.25 μA·cm^{-2} (N/n = 4/11; p = 0.016) (Table 5, Exp 2).

All solutions in these experiments contained a background of 70 mmol·l^{-1} of Na^+. Two further experiments were carried out in Na^+-free buffer, showing the same biphasic effects of menthol (Fig. 4b).

Effect of menthol on Na^+-induced currents

In the entire series of experiments, we avoided raising basolateral NH_4^+ concentration to unphysiological and potentially toxic levels. Accordingly, a chemical gradient for NH_4^+ was present. Two hypotheses were thus possible: (a) menthol stimulates ion channels within the epithelium, stimulating transcellular NH_4^+ flux, and (b) menthol initiates signaling with an impact on tight junctions, stimulating paracellular NH_4^+ flux. For this reason, the next series of experiments was performed with the same physiological NaCl buffer solution on both sides of the tissue. Since no chemical gradient was present as a driving force for paracellular transport, the stimulation of I_{sc} by menthol in these experiments clearly proves an effect on the transcellular passage of ions (Fig. 4c and Table 5, Exp 3). As before, a biphasic response was observed to a peak value by ΔI_{scPeak} = 6.95 ± 2.44 μA·cm^{-2} (N/n = 3/12; p < 0.05), with a subsequent continuous drop by ΔI_{scWash} = −13.91 ± 3.00 μA·cm^{-2} to a value significantly below zero (p = 0.016). Possibly, this negative current reflects a secretion of K^+ through nonselective cation channels opened by menthol.

Effect of thymol on NH_4^+-induced currents

Thymol is known to have stimulatory effects on TRPV3 [41, 59, 68]. In further experiments, the effect of thymol (1 mmol·l^{-1}) on NH_4^+-induced currents was tested in Na^+-free buffer. In five bovine tissues from four animals, the response resembled that observed with menthol, with a transient activation of current by ΔI_{scPeak} = 6.12 ± 1.99 μA·cm^{-2} (p < 0.001) followed by a subsequent reduction to ΔI_{scWash} = −10.43 ± 2.35 μA·cm^{-2}, significantly below the baseline (N/n = 4/5, p = 0.01, Fig. 5a). Four tissues from two further animals only showed this reduction (ΔI_{scWash} = −12.38 ± 4.89 μA·cm^{-2}, N/n = 2/4, p = 0.01, Fig. 5b). Despite a trend (p = 0.078), the transient activation of current level did not pass testing for significance when all data were pooled (Table 5, Exp 4). At a concentration of 100 μmol·l^{-1}, only subtle effects could be observed that again did not pass testing for significance (Table 5, Exp 5).

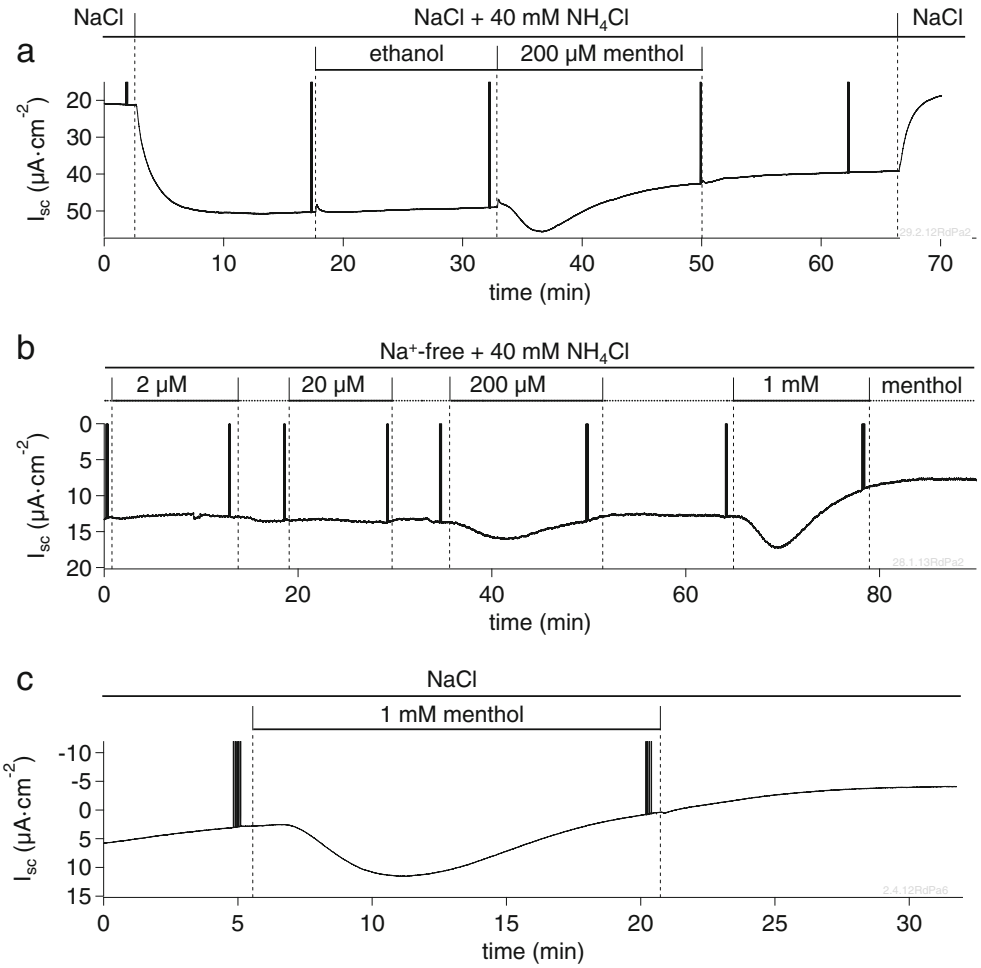

Fig. 4 Original recordings of bovine ruminal epithelium, measurement as in Fig. 3. **a** While in isolation, the solvant ethanol had no effect, menthol had modulatory effects on the NH_4^+-induced I_{sc}. **b** Effects of menthol on the NH_4^+-induced I_{sc} were concentration dependent and did not require the presence of Na^+ in the apical solution, which was replaced by $NMDG^+$. **c** A stimulation of I_{sc} by menthol could also be observed in a situation with an identical NaCl buffer on both sides, without any chemical gradient

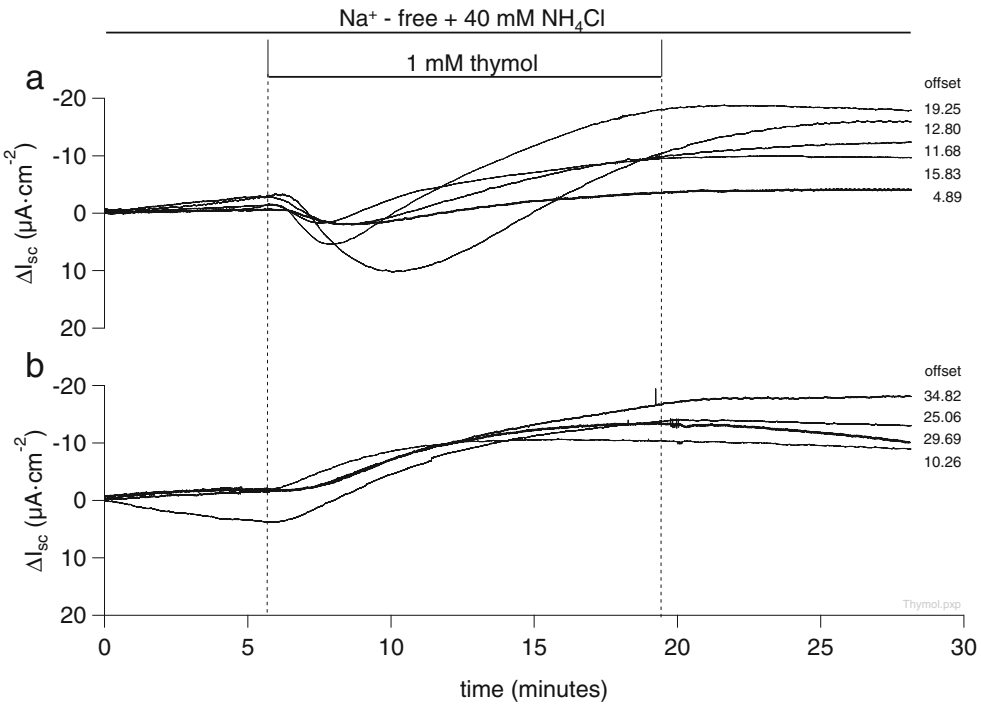

Fig. 5 Original recordings of bovine ruminal epithelia showing the effects of thymol in a Na^+-free NH_4^+ buffer solution, measured as in Fig. 3. To facilitate the graphic overlay of 11 separate recordings, the voltage pulses were removed via filtering and an offset current was subtracted from each curve as indicated on the right. **a** Original recordings from five epithelia from four individual animals, showing a biphasic response of I_{sc} after application of thymol. **b** Four epithelia from two different animals only showed a monophasic response (N/n = 2/4)

Table 5 Measurements of native bovine ruminal epithelium: effect of various TRP channel modulators on the short-circuit current (I_{sc}) (continuously perfused chamber)

Exp	Bath solutions			Short-circuit current I_{sc} ($\mu A \cdot cm^{-2}$)			N/n
	Buffer	Modulator	$\mu mol \cdot l^{-1}$	Before	Peak[a]	Wash[b]	
1	NH_4Cl	Menthol	1000	24.20 ± 4.51 a	28.73 ± 4.83 b	20.88 ± 3.68 a[c]	3/12
2	NH_4Cl	Menthol	200	30.99 ± 3.70 a	36.34 ± 3.66 b	26.42 ± 2.71 c	4/11
3	NaCl	Menthol	1000	00.90 ± 2.32 a	7.86 ± 4.05 b	−06.05 ± 1.99 c	3/12
4	NH_4Cl	Thymol	1000	08.39 ± 6.62 a	11.61 ± 6.95 a[c]	02.59 ± 5.55 b	6/9
5	NH_4Cl	Thymol	100	22.47 ± 3.87 a	22.19 ± 4.00 a	15.82 ± 9.60 a	2/4
6	NH_4Cl	Cinnam -aldehyde	1000	31.53 ± 3.15 a	28.39 ± 3.26 a[d]	28.30 ± 4.81 a	2/8
7	NH_4Cl	Capsaicin	100	23.10 ± 5.69 a	19.85 ± 5.33 b	21.54 ± 5.88 a	4/6
8	NH_4Cl (Na^+-free)	Menthyl Salicylate	1000	25.44 ± 1.80 a	21.06 ± 2.97 a	21.51 ± 4.09 a	3/4

Each row represents means ± SEM from a series of experiments in which one channel modulator was added to the mucosal buffer solution as indicated. Within rows, values with different lowercase letters are significantly different ($p < 0.05$, ANOVA, SNK)

[a] Maximal or minimal value of I_{sc} after addition of modulator

[b] Value measured 10 min after washout

[c] Trend for significant difference ($p < 0.1$, ANOVA, SNK) (see text)

[d] The power of the performed test was below the desired power; a difference may exist (see text)

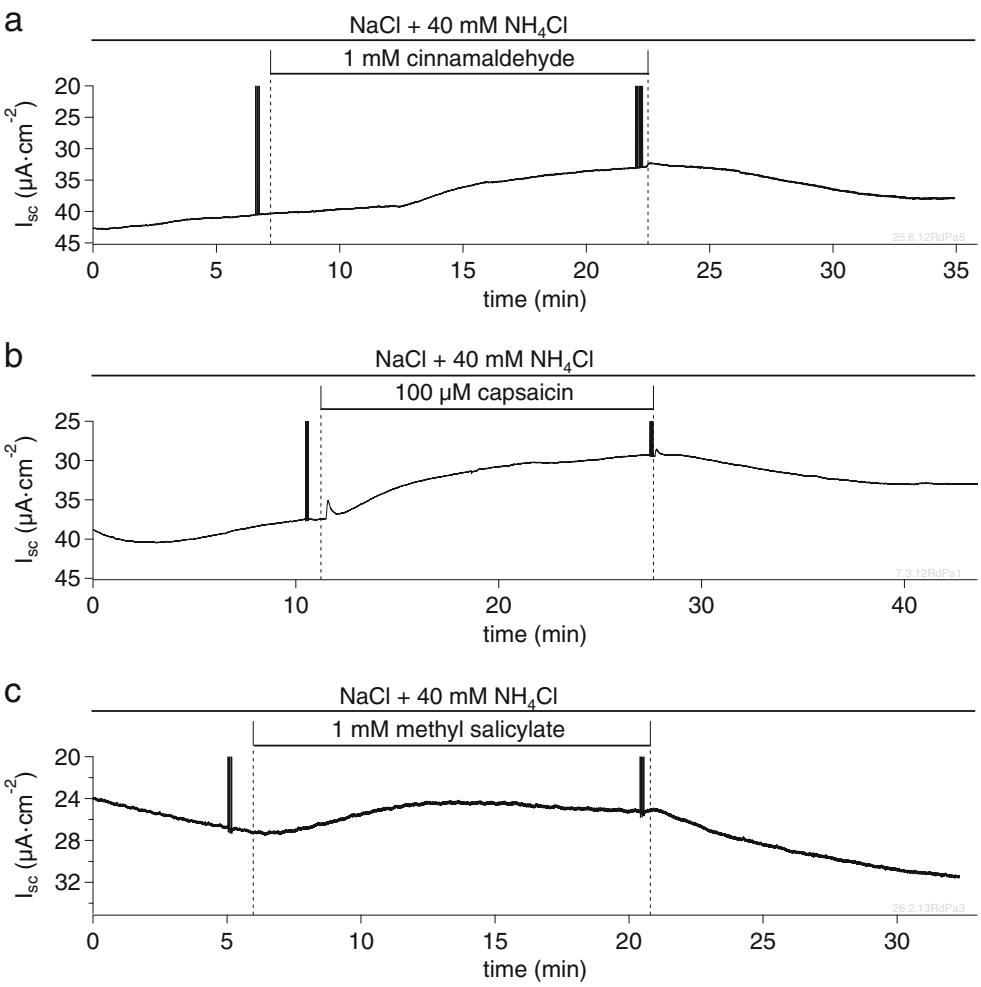

Fig. 6 Original recordings of bovine ruminal epithelium as in Fig. 3, showing the effects of cinnamaldehyde (**a**), capsaicin (**b**) and methyl salicylate (**c**). Details in text

Table 6 Measurements of native ovine ruminal epithelium: effect of menthol on the short-circuit current (I_{sc}), the conductance (G_t), and the flux of Ca^{2+} (Ussing chambers)

Menthol ($\mu mol \cdot l^{-1}$)	0	10	100	1000	N/n	*p* value
I_{sc} ($\mu Eq \cdot cm^{-2} \cdot h^{-1}$) (before)	0.86 ± 0.14 a	0.88 ± 0.16 a	0.93 ± 0.16 a	0.84 ± 0.16 a	4/18	0.675
I_{sc} ($\mu Eq \cdot cm^{-2} \cdot h^{-1}$) (after)	0.68 ± 0.14 a	0.81 ± 0.17 a	0.75 ± 0.12 a	0.41 ± 0.08 b	4/18	0.004
ΔI_{scPeak} [a] ($\mu Eq \cdot cm^{-2} \cdot h^{-1}$)	0.04 ± 0.01 a	0.05 ± 0.01 a	0.07 ± 0.02 a	0.51 ± 0.10 b	4/18	<0.001
G_t ($mS \cdot cm^{-2}$) (before)	5.20 ± 0.68 a	5.94 ± 0.83 a	5.33 ± 0.73 a	5.56 ± 0.83 a	4/18	0.138
G_t ($mS \cdot cm^{-2}$) (after)	5.74 ± 0.49 a	5.83 ± 0.55 a	6.18 ± 0.62 a	7.32 ± 0.70 b	4/18	<0.001
ΔG_{tPeak} [b] ($mS \cdot cm^{-2}$)	0.22 ± 0.04 a	0.34 ± 0.13 a	0.14 ± 0.03 a	0.64 ± 0.10 b	4/18	0.007
J_{ms} ($nmol \cdot cm^{-2} \cdot h^{-1}$) ($Ca^{2+}$)	15.03 ± 1.22 a	17.86 ± 0.79 a[c]	17.39 ± 1.77 a[c]	16.31 ± 1.64 a	4/9	0.296[c]
J_{sm} ($nmol \cdot cm^{-2} \cdot h^{-1}$) ($Ca^{2+}$)	6.42 ± 0.86 a	4.62 ± 0.73 b	6.04 ± 0.81 a	9.50 ± 1.41 c	4/9	0.010
J_{net} ($nmol \cdot cm^{-2} \cdot h^{-1}$) ($Ca^{2+}$)	8.60 ± 1.43 a	13.24 ± 0.91 b	11.35 ± 2.10 b	6.47 ± 1.01 a	4/9	0.004

Experiments were performed using Na^+ buffers (no chemical gradient, details see text). Within rows, values with different lowercase letters are significantly different ($p < 0.05$, ANOVA, SNK). Note that J (in $\mu eq \cdot cm^{-2} \cdot h^{-1}$) = Φt (in $\mu A \cdot cm^{-2}$)/26.80 ≈ G_t (in mS) (see "Methods")

[a] Size of I_{sc} peak after addition of agonist or solvant

[b] Simultaneous change in G_t (see Fig. 7a)

[c] The power of the performed test was below the desired power; a difference may exist (see text)

Effects of cinnamaldehyde, capsaicin, methyl salicylate, camphor, icilin, and capsazepine

Cinnamaldehyde is a modulator of TRPA1 [2], with both activation and inhibition reported depending on the concentration applied. Cinnamaldehyde (1 $mmol \cdot l^{-1}$) visibly inhibited NH_4^+-induced currents across bovine ruminal epithelium ($\Delta I_{scPeak} = -3.14 \pm 1.29$ $\mu A \cdot cm^{-2}$) (Table 5, Exp 6 and Fig. 6a).

Capsaicin is known as a specific TRPV1 agonist [13, 60]. Application of 100 $\mu mol \cdot l^{-1}$ to the mucosal standard NH_4^+ buffer solution resulted in a significant decrease in current ($\Delta I_{scPeak} = -3.25 \pm 1.16$ $\mu A \cdot cm^{-2}$; N/n = 4/6; $p < 0.05$) with subsequent washout (N/n = 4/6, Fig. 6b and Table 5, Exp 7).

Given in Na^+-free NH_4^+ buffer, the TRPA1 agonist methyl salicylate induced a clearly visible and reversible drop in I_{sc} that did not pass testing for significance at N/n = 3/4 (Fig. 6c).

Responses to application of camphor, an agonist of TRPA1, TRPV1, and TRPV3 channels, also showed clearly visible but highly variable responses, which overall did not pass testing for significance (N/n = 3/6). Icilin is known as a strong and highly specific agonist of TRPM8 channels. Given in a concentration of 100 $\mu mol \cdot l^{-1}$, it showed no visible effects on I_{sc} at N/n = 2/3. Capsazepine reportedly blocks TRPV1 and

Table 7 Measurements of native ovine ruminal epithelium: effect of thymol on the short-circuit current (I_{sc}), the conductance (G_t), and the flux of Ca^{2+} (Ussing chambers)

Thymol ($\mu mol\ l^{-1}$)	0	10	100	1000	N/n	*p* value
I_{sc} ($\mu Eq \cdot cm^{-2} \cdot h^{-1}$) (before)	0.91 ± 0.08 a	0.82 ± 0.07 a	0.93 ± 0.08 a	0.83 ± 0.08 a	3/18	0.601
I_{sc} ($\mu Eq \cdot cm^{-2} \cdot h^{-1}$) (after)	0.80 ± 0.14 a	0.86 ± 0.10 a	0.87 ± 0.11 a	0.08 ± 0.14 b	3/18	<0.001
ΔI_{scPeak} [a] ($\mu Eq \cdot cm^{-2} \cdot h^{-1}$)	0.11 ± 0.02 a	0.08 ± 0.01 a	0.32 ± 0.11 b	0.79 ± 0.20 c	3/18	0.001
G_t ($mS \cdot cm^{-2}$) (before)	3.85 ± 0.44 a	4.07 ± 0.52 a	3.95 ± 0.44 a	3.84 ± 0.47 a	3/18	0.452
G_t ($mS \cdot cm^{-2}$) (after)	3.84 ± 0.35 a	3.82 ± 0.41 a	3.91 ± 0.41 a	8.83 ± 0.54 b	3/18	<0.001
ΔG_{tPeak} [b] ($mS \cdot cm^{-2}$)	0.17 ± 0.03 a	0.20 ± 0.11 b	0.50 ± 0.13 c	0.72 ± 0.17 d	3/18	0.002
J_{ms} ($nmol \cdot cm^{-2} \cdot h^{-1}$) ($Ca^{2+}$)	13.95 ± 1.94 a	12.66 ± 1.87 a	13.52 ± 2.00 a	15.06 ± 1.50 b	4/9	0.024
J_{sm} ($nmol \cdot cm^{-2} \cdot h^{-1}$) ($Ca^{2+}$)	5.26 ± 0.38 a	3.63 ± 0.42 b	4.30 ± 0.48 ab	13.81 ± 1.25 c	4/9	<0.001
J_{net} ($nmol \cdot cm^{-2} \cdot h^{-1}$) ($Ca^{2+}$)	8.68 ± 1.68 a	9.03 ± 1.80 a	9.22 ± 1.98 a	1.95 ± 1.00 b	4/9	0.004

Experiments were performed using Na^+ buffers (no chemical gradient, details see text). Within rows, values with different lowercase letters are significantly different ($p < 0.05$, ANOVA, SNK). Note that J (in $\mu eq \cdot cm^{-2} \cdot h^{-1}$) = Φt (in $\mu A \cdot cm^{-2}$)/26.80 ≈ G_t (in mS) (see "Methods")

[a] Change to I_{sc} peak after addition of agonist or solvant

[b] Simultaneous change in G_t (Fig. 7a)

TRPM8. When tested on two epithelia at 20 μmol·l^{-1}, no effect on current was observed (N/n = 2/2).

Effects of menthol and thymol on the I_{sc}, the G_t, and on $^{45}Ca^{2+}$-fluxes across the ovine rumen

Given the well-known role of the ruminal epithelium in the absorption of Ca^{2+} [26, 47, 56], the effect of menthol and thymol on the flux of $^{45}Ca^{2+}$ was subsequently investigated in ovine epithelia in classical Ussing chambers. The ruminal epithelium of sheep, which represents an established model for transport across the rumen of cattle, can be more easily stripped from the submucosal layers so that tissue damage is less likely. All experiments were performed using a standard rumen buffer with SCFA but without NH_4^+ and gassed with 95 % O_2/CO_2 [56]. Since the concentrations of Na^+, K^+, and Cl^- were equal on both sides of the epithelium, any change in I_{sc} should reflect transcellular transport. Tissue conductance G_t was monitored throughout.

The values given in Tables 6 and 7 reflect measurements 5 min before and 80 min after application of the agonist (referred to as I_{sc} (before) and I_{sc} (after), and G_t (before) and G_t (after), respectively). In addition, the size of the maximal positive change in I_{sc} after application of the agonist (ΔI_{scPeak}) and the corresponding change in G_t (ΔG_{tPeak}) until that timepoint are given in the tables (Fig. 7a). Values of I_{sc} are given in μEq·cm^{-2}·h^{-1}, which allows a direct comparison with the G_t in mS·cm^{-2} (see "Methods"). To test for epithelial vitality, ouabain was given at the end of each experiment. The effect of menthol and thymol was tested in concentrations of 10, 100, and 1000 μmol·l^{-1} in paired tissues from the same animal versus an equivalent amount of the solvent (ethanol) (Table 6 and Table 7). Sixty minutes after application of the test substance, mucosal to serosal flux of $^{45}Ca^{2+}$ ($J_{ms}(Ca^{2+})$)

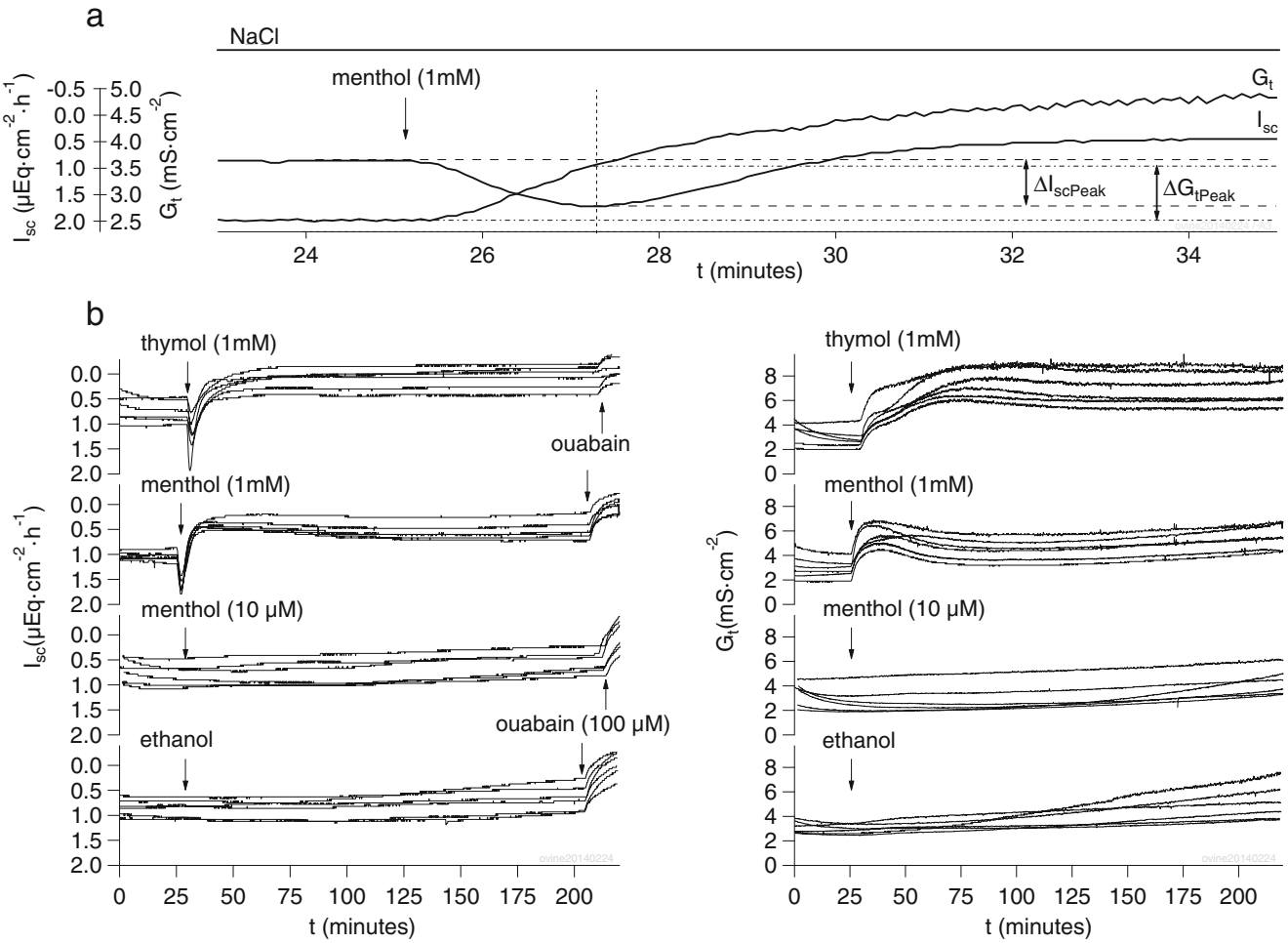

Fig. 7 Original recordings from pieces of ruminal epithelium from one sheep, measured in 24 conventional Ussing chambers in parallel (NaCl on both sides; no cation gradient). **a** Detail from one epithelium: after addition of menthol to the mucosal bath solution, a transient rise in I_{sc} (in μEq·cm^{-2}·h^{-1}) by ΔI_{scPeak} was observed that was coupled to an almost identical change in the conductance by ΔG_{tPeak} (in mS·cm^{-2}). **b** Overlay of the raw data from all 24 chambers with 6 epithelia in each treatment group (time relative to start of measurement in each individual chamber; no current offset). Note the difference in the G_t response of the epithelia to menthol and thymol, which may reflect significant differences in the pharmacological interaction of these agonists with the tissue

and serosal to mucosal flux of $^{45}Ca^{2+}$ ($J_{sm}(Ca^{2+})$) were measured for three flux periods of 30 min each. Values did not change significantly over time and were subsequently pooled to yield one mean value for that epithelium.

Figure 7 shows an additional experiment in which menthol and thymol were tested in parallel on the tissues of one further sheep. Since this experiment did not include data for all treatment groups, the data are not included in the tables or the statistics.

Menthol

As in bovine ruminal epithelia, application of menthol in a concentration of ≥100 μmol·l^{-1} led to a biphasic response in the level of I_{sc}, with an initial rise in I_{sc} by ΔI_{scPeak} (Table 6 and Fig. 7). The conductance G_t increased sharply in parallel to the I_{sc} value, with a mean change of ΔG_{tPeak} measured at the time of the I_{sc} peak (Fig. 7a). As before, I_{sc} subsequently declined to a value significantly lower than that measured initially for that epithelium, while G_t continued to rise. Application of ouabain (100 μmol·l^{-1}) led to a reduction of I_{sc} to a level not significantly different from zero. The value of G_t was not affected (Fig. 7).

The net absorption of Ca^{2+} ($J_{net}(Ca^{2+})$) increased significantly versus control after application of menthol at the two lower concentrations (Table 6). Two components contributed to this effect: Firstly, the two lower concentrations of menthol suppressed $J_{sm}(Ca^{2+})$ in a highly significant manner (ANOVA, $p < 0.001$). Secondly, there was a certain trend for a stimulation of $J_{ms}(Ca^{2+})$ by menthol. When values of $J_{ms}(Ca^{2+})$ were tested in isolation versus the control group (paired t test), p values of 0.088 and 0.043 emerged for concentrations of 10 or 100 μmol·l^{-1} menthol, respectively, although testing of all groups via ANOVA did not yield a reliable result (Table 6).

Thymol

Effects of thymol were similar to those seen with menthol, with a concentration dependent, significant biphasic response in I_{sc}, a monophasic increase in G_t, and corresponding responses to ouabain (Fig. 7 and Table 7). At a concentration of 1000 mmol·l^{-1}, thymol significantly stimulated both $J_{ms}(Ca^{2+})$ and $J_{sm}(Ca^{2+})$, resulting in a corresponding significant decline in $J_{net}(Ca^{2+})$ versus control. As in the case of menthol, thymol reduced $J_{sm}(Ca^{2+})$ at the two lower concentrations.

Identification of mRNA encoding for candidate genes from the TRP channel family

After amplification using the primers in Table 1, a strong signal for TRPA1, TRPV3, TRPV4, TRPM6, and TRPM7

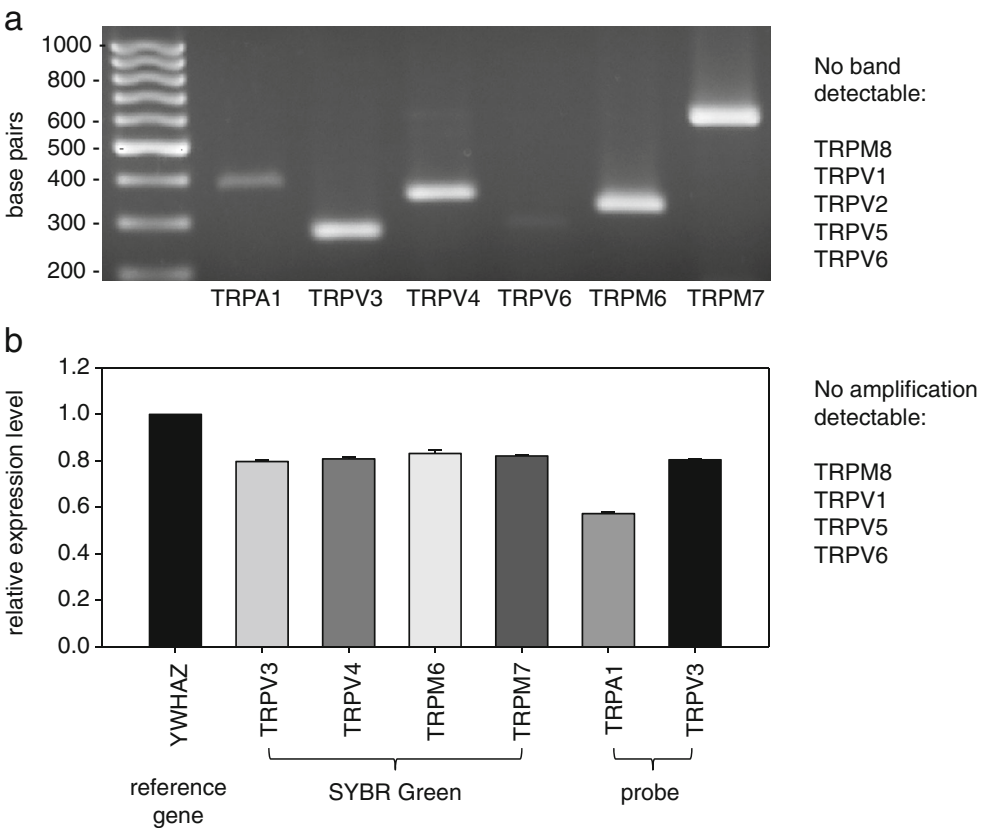

Fig. 8 **a** Gel electrophoresis loaded with PCR products from pooled cDNA from three cows using primers for TRPA1, V3, V4, V6, M6, and M7 (from *left* to *right*). Prominent bands were detected for target genes TRPA1, V3, V4, M6, and M7, indicating strong expression levels. Conversely, only discrete bands for TRPV6 emerged. **b** The figure shows the means (±SEM) of mRNA expression of ruminal samples from six individual cows, normalized to the reference gene YWHAZ. No significant differences emerged between the expression levels of TRPA1, V3, V4, V6, M6, and M7, although there was a clear trend for lower expression of TRPA1 versus all other channels. Any expression of TRPM8, TRPV1, TRPV5, and TRPV6 was below the detection threshhold (details: see text)

was detected in gel electrophoresis of both ovine and bovine samples, indicating a strong messenger RNA (mRNA) expression of the target genes by the ruminal epithelium (Fig. 8). TRPV6 was only very weakly expressed, while bands for TRPV1, TRPV5, and TRPM8 were only evident in bovine medulla oblongata, kidney, or testis, but not in the ovine or bovine ruminal epithelium (data not shown). It thus appears that any expression of TRPV1, TRPV5, or TRPM8 by the ruminal epithelium is either nonexistant or very discrete. For TRPV2, no reliable band was detected in either ruminal tissue or control tissues using two different primer sequences.

In the subsequent qPCR analysis, target gene expression of six animals was compared semiquantitatively using a SYBR Green setup. Relative to the housekeeping gene YWHAZ, the expression levels of TRPV3, V4, M6, and M7 were remarkably similar in all tissues studied (expression levels approximately 0.8-fold, Fig. 8). Expression of TRPV1, TRPV5, TRPV6, and TRPM8 was not detected, confirming the results of the PCR approach. The Ct values for TRPA1 exceeded 30 cycles and were considered insufficiently reliable. To ensure the validity of the results, a primer/probe setup was established for TRPA1 and TRPV3 relative to three housekeeping genes, among which YWHAZ emerged as the most stable (see "Methods"). Evaluation of the data showed that in every sample, the relation of TRPV3 and YWHAZ was nearly identical using both setups (average relation of mean Ct value YWHAZ/ mean Ct value TRPV3 = 0.80). Conversely, average TRPA1 expression was only 0.57-fold of YWHAZ, although this difference did not pass testing for significance.

Discussion

A channel-mediated uptake route for ammonia in the form of NH_4^+ from the rumen has been postulated for over a decade [1, 10], but both the molecular identity of these channels and that of the divalent nonselective cation channels that mediate the uptake of Na^+ by the ruminal epithelium have remained obscure [31]. In the current study, we provide functional and molecular biological evidence for the involvement of members of the TRP channel family in the uptake of NH_4^+, Na^+, and Ca^{2+}. The functional effects of specific modulators point toward TRPV3 and TRPA1 as prime candidates. This result is supported by the finding that both channels are expressed on the level of mRNA in ovine (PCR) and bovine (PCR, qPCR) samples. However, it should be stressed that other TRP channels, in particular TRPV4, are robustly expressed at the level of mRNA in both sheep and cattle. While a functional significance for transport remains to be demonstrated, these channels may play additional roles. For both species, we further confirm that any ruminal expression of mRNA encoding for TRPV6 is very weak [63, 64], while no bands for TRPM8, TRPV1, TRPV2, or TRPV5 were detectable. Finally, we demonstrate that, in addition to the ubiquitous Mg^{2+} channel TRPM7 previously identified in sheep [50], both the ovine and the bovine rumen express mRNA encoding for the epithelial Mg^{2+} channel TRPM6.

In a first step, we demonstrate that, as previously shown for the ovine rumen [1, 10] and the porcine cecum [54], application of NH_4^+ increased both the transepithelial potential and the short-circuit current across the bovine ruminal epithelium (Figs. 2 and 3, Tables 3 and 4). The NH_4^+-induced I_{sc} persisted after replacement of all Na^+ by $NMDG^+$, which suggests that basolateral efflux may also involve NH_4^+ via a mechanism that remains to be clarified. Since protons are removed from the rumen together with ammonia, the large losses of NH_4^+ from the rumen of cattle fed high concentrate diets may represent a strategy that helps the animals to cope with the acidotic ruminal pH value that typically develops in this feeding scenario [29].

Transcellular transport of NH_4^+ is supported not only by the blocking effect of the nonselective cation channel blocker verapamil but also by the results of experiments using pH-selective electrodes, showing that as in sheep, exposure to NH_4^+ depolarizes the apical membrane and acidifies the cytosol [33] (Fig. 2 and Table 3). Since the cytosol is more alkaline than the apical solution (~6.4), a certain fraction of the NH_4^+ that enters will deprotonate to NH_3 and leave in that form. In line with this, a previous study has shown that exposure to NH_4^+ stimulates Na^+ uptake via NHE, with the stimulatory effect blockable by amiloride [1]. An apical recirculation of ammonia (in as NH_4^+, out apically as NH_3) is conceivable and may explain why the stimulation of Na^+ transport via NHE exceeded the total net transport of ammonia in that study.

There is currently no reason to believe that chloride secretion as seen in the colon contributes significantly to the I_{sc} across the ruminal epithelium. Thus, bumetanide, which blocks Na^+-K^+-$2Cl^-$ transport, had no effect in this study, while past attempts to stimulate CFTR by elevating cAMP have failed [16, 67]. Current models suggest that chloride is absorbed by the rumen via an electrically silent process [35] that involves apical Cl^-/HCO_3^- exchange coupled to Na^+/H^+ exchange [3, 20] and basolateral efflux via an anion channel [20, 45, 55], driven by the Na^+/K^+-ATPase.

A central clue toward identifying the apical uptake pathway for NH_4^+ comes from the observation that both in bovine tissues and in isolated cells in patch clamp experiments, the NH_4^+-induced current could be strongly enhanced by removal of Ca^{2+} and Mg^{2+} (Figs. 1 and 3, Tables 2 and 4). In the patch clamp experiments and as previously observed [1], application of NH_4^+–gluconate stimulated not only influx of NH_4^+ at −120 mV but also efflux of K^+ or Na^+ from the pipette solution at +100 mV. Such effects are typically seen when a permeant ion enters the pore of a multi-ion channel [24] and suggests that K^+, Na^+, and NH_4^+ permeate the pore of a joint nonselective cation channel. As previously observed for Na^+

and K^+ [31], the block by divalent cations (Ca^{2+}, Mg^{2+}) was voltage dependent, with effects maximal at −120 mV. In conjunction, these observations argue for a permeation of NH_4^+ through the pore of a nonselective cation channel with characteristics resembling those of the TRP family [40].

In further attempts to characterize the NH_4^+ conductance of the native ruminal epithelium, menthol and thymol emerged as potent agonists eliciting a biphasic current response when applied in solutions containing either cation. Menthol is known for its specific effects on TRPM8 [5], TRPV3 [59], and TRPA1 [28], and thymol primarily for its stimulatory effects on TRPV3 [41, 59, 68]. Of these candidate genes, only TRPA1 and TRPV3 were expressed by the rumen at the level of mRNA, excluding TRPM8 as a potential candidate. This finding is supported by the lack of a functional effect of the tissue in response to the TRPM8 agonist icilin. Both TRPA1 and TRPV3 discriminate poorly between different cations, with competition between monovalent and divalent cations in the channel pore leading to an apparent "block" of the monovalent current.

A closer look at the effects of menthol and thymol reveals interesting insights. Applied apically at a concentration ≥100 μmol·l^{-1} and in solutions containing either NH_4^+ or Na^+ or both, menthol or thymol induced a biphasic activation of short-circuit current with an initial stimulation to a peak value followed by a decline to values below the original level. It may be argued that since the mobility for NH_4^+ (~1) is higher than that of Na^+ (0.682) [6], the current peak reflects a transient opening of the paracellular pathway with paracellular efflux of NH_4^+. However, in experiments with Na^+, no chemical gradient was present so that an opening of the paracellular pathway should have resulted in a drop in current rather than a rise. Instead, the same current profile was observed, arguing for the opening of a channel.

Several different explanations are possible for the biphasic response. Since a thick stratum corneum covers the apical, transporting layer of cells in the rumen, the current profile may reflect a gradual increase in the concentration of the agonist, with an initial stimulation by low concentrations followed by subsequent inhibitory effects [2, 28]. If this were the case, only the stimulatory effect should have been seen at lower concentrations of the agonist, which was not the case. Alternately, time-dependent desensitization may have occurred, as reported after short-term exposure of a cell line expressing TRPV3 [51]. A third hypothesis is possible: An initial stimulation of Na^+ or NH_4^+ influx into the epithelium with depolarization of the apical membrane is followed by a gradual increase in the efflux of K^+ through the nonselective pore, leading to an inversion of the direction of current in our experiments. With due caution, this interpretation is supported by the observation that after the initial menthol-induced peak, the I_{sc} values of bovine epithelia in symmetrical NaCl Ringer declined to values significantly below zero (Table 5, Exp. 3), while tissue conductance continued to rise (Tables 6 and 7, Fig. 7).

The last series of experiments was performed using sheep ruminal epithelia incubated in conventional Ussing chambers (Tables 6 and 7, Fig. 7). As before, we observed a marked change in I_{sc} (ΔI_{scPeak}) at the two higher concentrations of both menthol and thymol, as discussed above. Since Na^+ was in equilibrium across the tissue in these experiments, the menthol-induced peak is clearly caused by transcellular processes. In parallel to ΔI_{scPeak}, a rise in G_t (by ΔG_{tPeak}) was observed (Fig. 7a). An old electrophysiological "rule of the thumb" states that at 37 °C, the flux of an ion (in μeq·cm^{-2}·h^{-1}) is numerically identical to the conductance (in mS·cm^{-2}) (for derivation, see "Methods"). At the highest concentration applied, ΔG_{tPeak} thus corresponds almost completely to ΔI_{scPeak} and consequently appears to primarily reflect current through a transcellular pathway.

The ruminal epithelium also contributes to the gastrointestinal absorption of Ca^{2+} in the ruminant. Carefully done recent studies of Ca^{2+} transport across the ovine rumen clearly show that mucosal to serosal flux of Ca^{2+} ($J_{ms}(Ca^{2+})$) is primarily transcellular [64] and involves both electroneutral and electrogenic mechanisms [65]. However, as confirmed in this study, attempts to detect mRNA encoding for the classical epithelial Ca^{2+} channels TRPV5 and TRPV6 were not successful [48, 63, 64].

TRPA1 and TRPV3 both have a considerable conductance for Ca^{2+}, with values of $p(Ca^{2+})/p(Na^+)$ in the range of 7 to 10 and 1 to 12 for TRPV3 and TRPA1, respectively [19, 38, 69], with an influx of Ca^{2+} observable after stimulation with appropriate agonists [21]. Accordingly, the effects of menthol and thymol on Ca^{2+} fluxes were studied. At the two lower concentrations applied, menthol tended to increase $J_{ms}(Ca^{2+})$, with effects approaching significance level in paired testing versus control tissues. The significant effect of 1000 μmol l^{-1} thymol on $J_{ms}(Ca^{2+})$ may reflect an action on both transcellular and paracellular pathways. Somewhat unexpectedly, the serosal to mucosal flux of $^{45}Ca^{2+}$ ($J_{sm}(Ca^{2+})$) dropped significantly after application of either menthol or thymol at the lowest concentration (10 μmol·l^{-1}). Since ruminal $J_{sm}(Ca^{2+})$ has been shown to correlate significantly to the flux of mannitol as a marker of paracellular transport [64], the most likely explanation for this observation is a closing of the paracellular pathway. In conjunction, the two lower concentrations of menthol (10 and 100 μmol·l^{-1}) significantly enhanced the net absorption of Ca^{2+} by the ruminal epithelium, via mechanisms that probably involve both a direct action on TRP channels and secondary effects on barrier-forming proteins of the paracellular pathway. Both effects may be linked, since a number of studies have shown that calcium entry through TRP channels modulates barrier integrity [9, 44, 57]. An involvement of TRPA1 or TRPV3 and possibly TRPV4 in the apical uptake of Ca^{2+} should thus be considered, although further work is clearly warranted.

Acknowledgments Financial support for this study came from the Forschungskommission of the Freie Universität Berlin and from the European Social Fund (ESF) and the German Ministry of Economics and Technology based on a decision of the German Parliament (Projektträger Jülich 03EFABE057). In the latter part of the study, Katharina Schrapers (née Hille) was supported by the "Akademie für Tiergesundheit." The expert technical help of Gisela Manz, Susanne Trappe, Martin Grunau, Uwe Tietjen, and last but certainly not least, Katharina Wolf is gratefully acknowledged.

Compliance with ethical standards

Disclosure This study was performed for purely scientific reasons within a conventional academic framework but has recently led to a patent that is pending (involving the authors Friederike Stumpff and Julia Rosendahl, both as employees of the Freie Universität) and a start-up company supported by "Exist" and the Freie Universität Berlin. The company is owned by Julia Rosendahl, Hannah Braun, Katharina Schrapers, and Friederike Stumpff. This publication will have no impact on the commercial success or failure of that enterprise, and there is no conflict of interest.

Some preliminary results were published in the form of abstracts and a thesis (Julia Rosendahl).

References

1. Abdoun K, Stumpff F, Wolf K, Martens H (2005) Modulation of electroneutral Na transport in sheep rumen epithelium by luminal ammonia. Am J Physiol Gastrointest Liver Physiol 289:G508–G520. doi:10.1152/ajpgi.00436.2004
2. Alpizar YA, Gees M, Sanchez A, Apetrei A, Voets T, Nilius B, Talavera K (2013) Bimodal effects of cinnamaldehyde and camphor on mouse TRPA1. Pflugers Arch 465:853–864. doi:10.1007/s00424-012-1204-x
3. Aschenbach JR, Bilk S, Tadesse G, Stumpff F, Gäbel G (2009) Bicarbonate-dependent and bicarbonate-independent mechanisms contribute to nondiffusive uptake of acetate in the ruminal epithelium of sheep. Am J Physiol Gastrointest Liver Physiol 296:G1098–G1107. doi:10.1152/ajpgi.90442.2008
4. Aschenbach JR, Penner GB, Stumpff F, Gabel G (2011) Ruminant nutrition symposium: role of fermentation acid absorption in the regulation of ruminal pH. J Anim Sci 89:1092–1107. doi:10.2527/jas.2010-3301
5. Bandell M, Dubin AE, Petrus MJ, Orth A, Mathur J, Hwang SW, Patapoutian A (2006) High-throughput random mutagenesis screen reveals TRPM8 residues specifically required for activation by menthol. Nat Neurosci 9:493–500. doi:10.1038/nn1665
6. Barry PH (2012) Ionic mobility tables. http://web.med.unsw.edu.au/phbsoft/mobility_listings.htm
7. Barry PH, Lynch JW (1991) Liquid junction potentials and small cell effects in patch-clamp analysis. J Membr Biol 121:101–117. doi:10.1007/BF01870526
8. Behera SN, Sharma M, Aneja VP, Balasubramanian R (2013) Ammonia in the atmosphere: a review on emission sources, atmospheric chemistry and deposition on terrestrial bodies. Environ Sci Pollut Res Int 20:8092–8131. doi:10.1007/s11356-013-2051-9
9. Blaydon DC, Kelsell DP (2014) Defective channels lead to an impaired skin barrier. J Cell Sci 127:4343–4350. doi:10.1242/jcs.154633
10. Bödeker D, Kemkowski J (1996) Participation of NH4+ in total ammonia absorption across the rumen epithelium of sheep (Ovis aries). Comp Biochem Physiol A Physiol 114:305–310. doi:10.1016/0300-9629(96)00012-6
11. Boron WF (2010) Sharpey-Schafer lecture: gas channels. Exp Physiol 95:1107–1130. doi:10.1113/expphysiol.2010.055244
12. Bouwman AF, Lee DS, Asman WAH, Dentener FJ, Van Der Hoek KW, Olivier JGJ (1997) A global high-resolution emission inventory for ammonia. Glob Biogeochem Cycles 11:561–587. doi:10.1029/97gb02266
13. Caterina MJ, Schumacher MA, Tominaga M, Rosen TA, Levine JD, Julius D (1997) The capsaicin receptor: a heat-activated ion channel in the pain pathway. Nature 389:816–824. doi:10.1038/39807
14. Damann N, Voets T, Nilius B (2008) TRPs in our senses. Curr Biol 18:R880–R889. doi:10.1016/j.cub.2008.07.063
15. Delgado-Elorduy A, Theurer CB, Huber JT, Alio A, Lozano O, Sadik M, Cuneo P, De Young HD, Simas IJ, Santos JE, Nussio L, Nussio C, Webb KE Jr, Tagari H (2002) Splanchnic and mammary nitrogen metabolism by dairy cows fed dry-rolled or steam-flaked sorghum grain. J Dairy Sci 85:148–159. doi:10.3168/jds.S0022-0302(02)74063-0
16. Gäbel G, Butter H, Martens H (1999) Regulatory role of cAMP in transport of Na+, Cl- and short-chain fatty acids across sheep ruminal epithelium. Exp Physiol 84:333–345. doi:10.1111/j.1469-445X.1999.01758.x
17. Galfi P, Neogrady S, Kutas F (1981) Culture of epithelial cells from bovine ruminal mucosa. Vet Res Commun 4:295–300. doi:10.1007/BF02278507
18. Gärtner K, von Engelhardt W (1964) Experiments concerning the resorption mechanism of ammonia through the ruminal mucosa of ruminants. Dtsch Tierarztl Wochenschr 71:57–60
19. Gees M, Colsoul B, Nilius B (2010) The role of transient receptor potential cation channels in Ca2+ signaling. Cold Spring Harb Perspect Biol 2:a003962. doi:10.1101/cshperspect.a003962
20. Georgi MI, Rosendahl J, Ernst F, Gunzel D, Aschenbach JR, Martens H, Stumpff F (2014) Epithelia of the ovine and bovine forestomach express basolateral maxi-anion channels permeable to the anions of short-chain fatty acids. Pflugers Arch 466:1689–1712. doi:10.1007/s00424-013-1386-x
21. Grubisha O, Mogg AJ, Sorge JL, Ball LJ, Sanger H, Ruble CL, Folly EA, Ursu D, Broad LM (2014) Pharmacological profiling of the TRPV3 channel in recombinant and native assays. Br J Pharmacol 171:2631–2644. doi:10.1111/bph.12303
22. Handlogten ME, Hong SP, Zhang L, Vander AW, Steinbaum ML, Campbell-Thompson M, Weiner ID (2005) Expression of the ammonia transporter proteins Rh B glycoprotein and Rh C glycoprotein in the intestinal tract. Am J Physiol Gastrointest Liver Physiol 288:G1036–G1047. doi:10.1152/ajpgi.00418.2004
23. Harmeyer J, Martens H (1980) Aspects of urea metabolism in ruminants with reference to the goat. J Dairy Sci 63:1707–1728. doi:10.3168/jds.S0022-0302(80)83132-8
24. Hille B (2001) Ion Channels of Excitable Membranes. 3rd edn. Sinauer Associates, Sunderland, Mass. doi:ISBN 978–0878933211
25. Hodgkin AL (1951) The ionic basis of electrical activity in nerve and muscle. Biol Rev 26:339–409. doi:10.1111/j.1469-185X.1951.tb01204.x
26. Höller H, Breves G, Kocabatmaz M, Gerdes H (1988) Flux of calcium across the sheep rumen wall in vivo and in vitro. Q J Exp Physiol 73:609–618
27. Hsu YJ, Hoenderop JG, Bindels RJ (2007) TRP channels in kidney disease. Biochim Biophys Acta 1772:928–936. doi:10.1016/j.bbadis.2007.02.001
28. Karashima Y, Damann N, Prenen J, Talavera K, Segal A, Voets T, Nilius B (2007) Bimodal action of menthol on the transient receptor potential channel TRPA1. J Neurosci 27:9874–9884. doi:10.1523/JNEUROSCI.2221-07.2007

29. Kleen JL, Upgang L, Rehage J (2013) Prevalence and consequences of subacute ruminal acidosis in German dairy herds. Acta Vet Scand 55:48. doi:10.1186/1751-0147-55-48
30. Leonhard-Marek S (2002) Divalent cations reduce the electrogenic transport of monovalent cations across rumen epithelium. J Comp Physiol B 172:635–641. doi:10.1007/s00360-002-0292-x
31. Leonhard-Marek S, Stumpff F, Brinkmann I, Breves G, Martens H (2005) Basolateral Mg2+/Na + exchange regulates apical nonselective cation channel in sheep rumen epithelium via cytosolic Mg2+. Am J Physiol Gastrointest Liver Physiol 288:G630–G645. doi:10.1152/ajpgi.00275.2004
32. Li H, Sheppard DN, Hug MJ (2004) Transepithelial electrical measurements with the Ussing chamber. J Cyst Fibros 3(Suppl 2):123–126. doi:10.1016/j.jcf.2004.05.026
33. Lu Z, Stumpff F, Deiner C, Rosendahl J, Braun H, Abdoun K, Aschenbach JR, Martens H (2014) Modulation of sheep ruminal urea transport by ammonia and pH. Am J Physiol Regul Integr Comp Physiol 307:R558–R570. doi:10.1152/ajpregu.00107.2014
34. Marini AM, Matassi G, Raynal V, Andre B, Cartron JP, Cherif-Zahar B (2000) The human Rhesus-associated RhAG protein and a kidney homologue promote ammonium transport in yeast. Nat Genet 26:341–344. doi:10.1038/81656
35. Martens H, Gäbel G, Strozyk B (1991) Mechanism of electrically silent Na and Cl transport across the rumen epithelium of sheep. Exp Physiol 76:103–114. doi:10.1113/expphysiol.1991.sp00347
36. Montell C, Rubin GM (1989) Molecular characterization of the Drosophila trp locus: a putative integral membrane protein required for phototransduction. Neuron 2:1313–1323. doi:10.1016/0896-6273(89)90069-X
37. Musa-Aziz R, Chen LM, Pelletier MF, Boron WF (2009) Relative CO2/NH3 selectivities of AQP1, AQP4, AQP5, AmtB, and RhAG. Proc Natl Acad Sci U S A 106:5406–5411. doi:10.1073/pnas.0813231106
38. Nilius B, Prenen J, Owsianik G (2011) Irritating channels: the case of TRPA1. J Physiol 589:1543–1549. doi:10.1113/jphysiol.2010.200717
39. Nilius B, Szallasi A (2014) Transient receptor potential channels as drug targets: from the science of basic research to the art of medicine. Pharmacol Rev 66:676–814. doi:10.1124/pr.113.008268
40. Owsianik G, Talavera K, Voets T, Nilius B (2006) Permeation and selectivity of TRP channels. Annu Rev Physiol 68:685–717. doi:10.1146/annurev.physiol.68.040204.101406
41. Palazzo E, Rossi F, de Novellis V, Maione S (2013) Endogenous modulators of TRP channels. Curr Top Med Chem 13:398–407. doi:10.2174/1568026611313030014
42. Peier AM, Moqrich A, Hergarden AC, Reeve AJ, Andersson DA, Story GM, Earley TJ, Dragoni I, McIntyre P, Bevan S, Patapoutian A (2002) A TRP channel that senses cold stimuli and menthol. Cell 108:705–715. doi:10.1016/S0092-8674(02)00652-9
43. Ramsey IS, Delling M, Clapham DE (2006) An introduction to TRP channels. Annu Rev Physiol 68:619–647. doi:10.1146/annurev.physiol.68.040204.100431
44. Reiter B, Kraft R, Günzel D, Zeissig S, Schulzke JD, Fromm M, Harteneck C (2006) TRPV4-mediated regulation of epithelial permeability. FASEB J 20:1802–1812. doi:10.1096/fj.06-5772com
45. Sabirov RZ, Merzlyak PG, Islam MR, Okada T, Okada Y (2016) The properties, functions, and pathophysiology of maxi-anion channels. Pflugers Arch. doi:10.1007/s00424-015-1774-5
46. Saparov SM, Liu K, Agre P, Pohl P (2007) Fast and selective ammonia transport by aquaporin-8. J Biol Chem 282:5296–5301. doi:10.1074/jbc.M609343200
47. Schröder B, Rittmann I, Pfeffer E, Breves G (1997) In vitro studies on calcium absorption from the gastrointestinal tract in small ruminants. J Comp Physiol B 167:43–51
48. Schroder B, Wilkens MR, Ricken GE, Leonhard-Marek S, Fraser DR, Breves G (2015) Calcium transport in bovine rumen epithelium as affected by luminal Ca concentrations and Ca sources. Physiol Rep 3. doi:10.14814/phy2.12615
49. Schultheiss G, Martens H (1999) Ca-sensitive Na transport in sheep omasum. Am J Physiol 276:G1331–G1344. doi:10.1152/ajpgi.90532.2008
50. Schweigel M, Kolisek M, Nikolic Z, Kuzinski J (2008) Expression and functional activity of the Na/Mg exchanger, TRPM7 and MagT1 are changed to regulate Mg homeostasis and transport in rumen epithelial cells. Magnes Res 21:118–123
51. Sherkheli MA, Benecke H, Doerner JF, Kletke O, Vogt-Eisele AK, Gisselmann G, Hatt H (2009) Monoterpenoids induce agonist-specific desensitization of transient receptor potential vanilloid-3 (TRPV3) ion channels. J Pharm Pharm Sci 12:116–128
52. Stevens CE, Hume ID (1998) Contributions of microbes in vertebrate gastrointestinal tract to production and conservation of nutrients. Physiol Rev 78:393–427
53. Stokstad E (2014) Air pollution. Ammonia pollution from farming may exact hefty health costs. Science 343:238. doi:10.1126/science.343.6168.238
54. Stumpff F, Lodemann U, Van Kessel AG, Pieper R, Klingspor S, Wolf K, Martens H, Zentek J, Aschenbach JR (2013) Effects of dietary fibre and protein on urea transport across the cecal mucosa of piglets. J Comp Physiol B 183:1053–1063. doi:10.1007/s00360-013-0771-2
55. Stumpff F, Martens H, Bilk S, Aschenbach JR, Gäbel G (2009) Cultured ruminal epithelial cells express a large-conductance channel permeable to chloride, bicarbonate, and acetate. Pflugers Arch 457:1003–1022
56. Uppal SK, Wolf K, Martens H (2003) The effect of short chain fatty acids on calcium flux rates across isolated rumen epithelium of hay-fed and concentrate-fed sheep. J Anim Physiol Anim Nutr (Berl) 87:12–20
57. Villalta PC, Townsley MI (2013) Transient receptor potential channels and regulation of lung endothelial permeability. Pulm Circ 3:802–815. doi:10.1086/674765
58. Voets T, Janssens A, Prenen J, Droogmans G, Nilius B (2003) Mg2 + −dependent gating and strong inward rectification of the cation channel TRPV6. J Gen Physiol 121:245–260
59. Vogt-Eisele AK, Weber K, Sherkheli MA, Vielhaber G, Panten J, Gisselmann G, Hatt H (2007) Monoterpenoid agonists of TRPV3. Br J Pharmacol 151:530–540. doi:10.1038/sj.bjp.0707245
60. Vriens J, Nilius B, Vennekens R (2008) Herbal compounds and toxins modulating TRP channels. Curr Neuropharmacol 6:79–96. doi:10.2174/157015908783769644
61. Weiner ID (2004) The Rh gene family and renal ammonium transport. Curr Opin Nephrol Hypertens 13:533–540
62. Weiner ID, Verlander JW (2014) Ammonia transport in the kidney by Rhesus glycoproteins. Am J Physiol Renal Physiol 306:F1107–F1120. doi:10.1152/ajprenal.00013.2014
63. Wilkens MR, Kunert-Keil C, Brinkmeier H, Schröder B (2009) Expression of calcium channel TRPV6 in ovine epithelial tissue. Vet J 182:294–300. doi:10.1016/j.tvjl.2008.06.020
64. Wilkens MR, Mrochen N, Breves G, Schröder B (2011) Gastrointestinal calcium absorption in sheep is mostly insensitive to an alimentary induced challenge of calcium homeostasis. Comp Biochem Physiol B Biochem Mol Biol 158:199–207. doi:10.1016/j.cbpb.2010.11.008
65. Wilkens MR, Praechter C, Breves G, Schröder B (2015) Stimulating effects of a diet negative in dietary cation-anion difference on calcium absorption from the rumen in sheep. J Anim Physiol Anim Nutr (Berl). doi:10.1111/jpn.12296
66. Winkler FK (2006) Amt/MEP/Rh proteins conduct ammonia. Pflugers Arch 451:701–707
67. Wolffram S, Frischknecht R, Scharrer E (1989) Influence of theophylline on the electrical potential difference and ion fluxes (Na,

Cl, K) across the isolated rumen epithelium of sheep. Zentralbl Veterinarmed A 36:755–762

68. Xu H, Delling M, Jun JC, Clapham DE (2006) Oregano, thyme and clove-derived flavors and skin sensitizers activate specific TRP channels. Nat Neurosci 9:628–635. doi:10.1038/nn1692

69. Xu H, Ramsey IS, Kotecha SA, Moran MM, Chong JA, Lawson D, Ge P, Lilly J, Silos-Santiago I, Xie Y, DiStefano PS, Curtis R, Clapham DE (2002) TRPV3 is a calcium-permeable temperature-sensitive cation channel. Nature 418:181–186. doi:10.1038/nature00882